Dissertation Defense: "^{129}Xe Relaxation and Rabi Oscillations"

Mark Limes

Oct. 30th, 2013

THE UNIVERSITY OF UTAH

Magnetic Resonance (MR)

– Energy difference (Zeeman) is "resonated" by applying an oscillating field

$\boldsymbol{\mu}_S = \gamma \mathbf{S}/\hbar$ $\quad -\boldsymbol{\mu}_S \cdot \mathbf{B} \to E$ $\quad E_\downarrow - E_\uparrow = \hbar\omega_0$

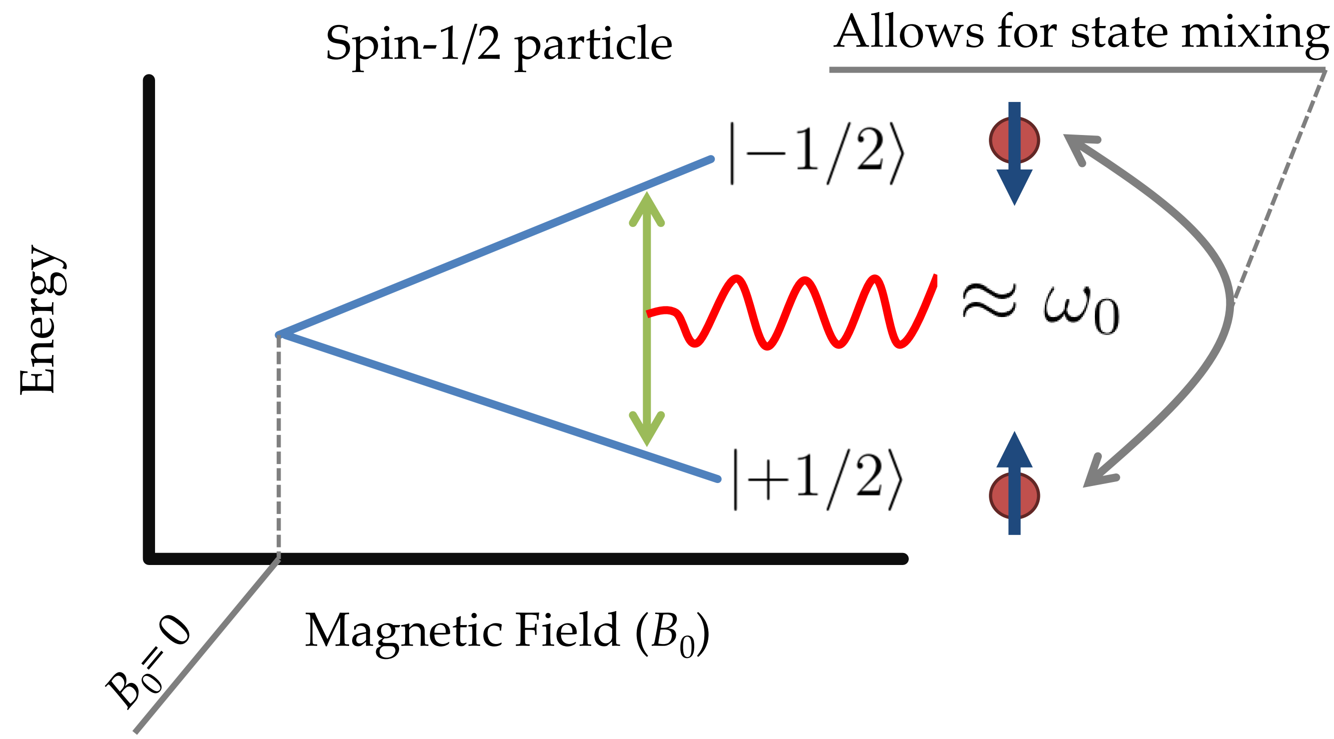

Magnetic Resonance (MR)

– For most MR exp., an oscillating field is perpendicular to a larger, quantizing field

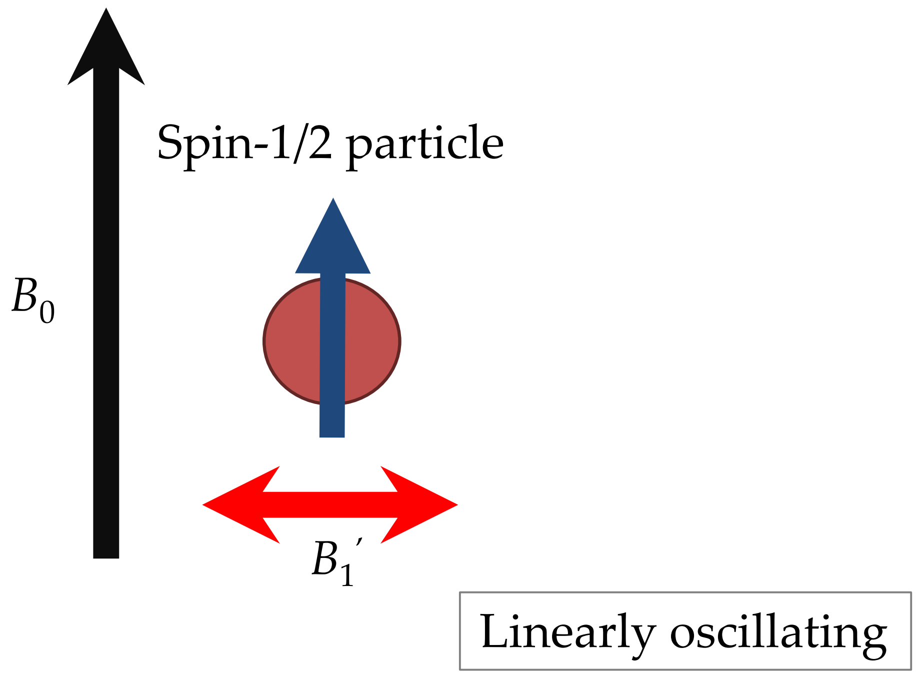

Magnetic Resonance (MR)

– The linear B_1' field can be decomposed as two counter-rotating components

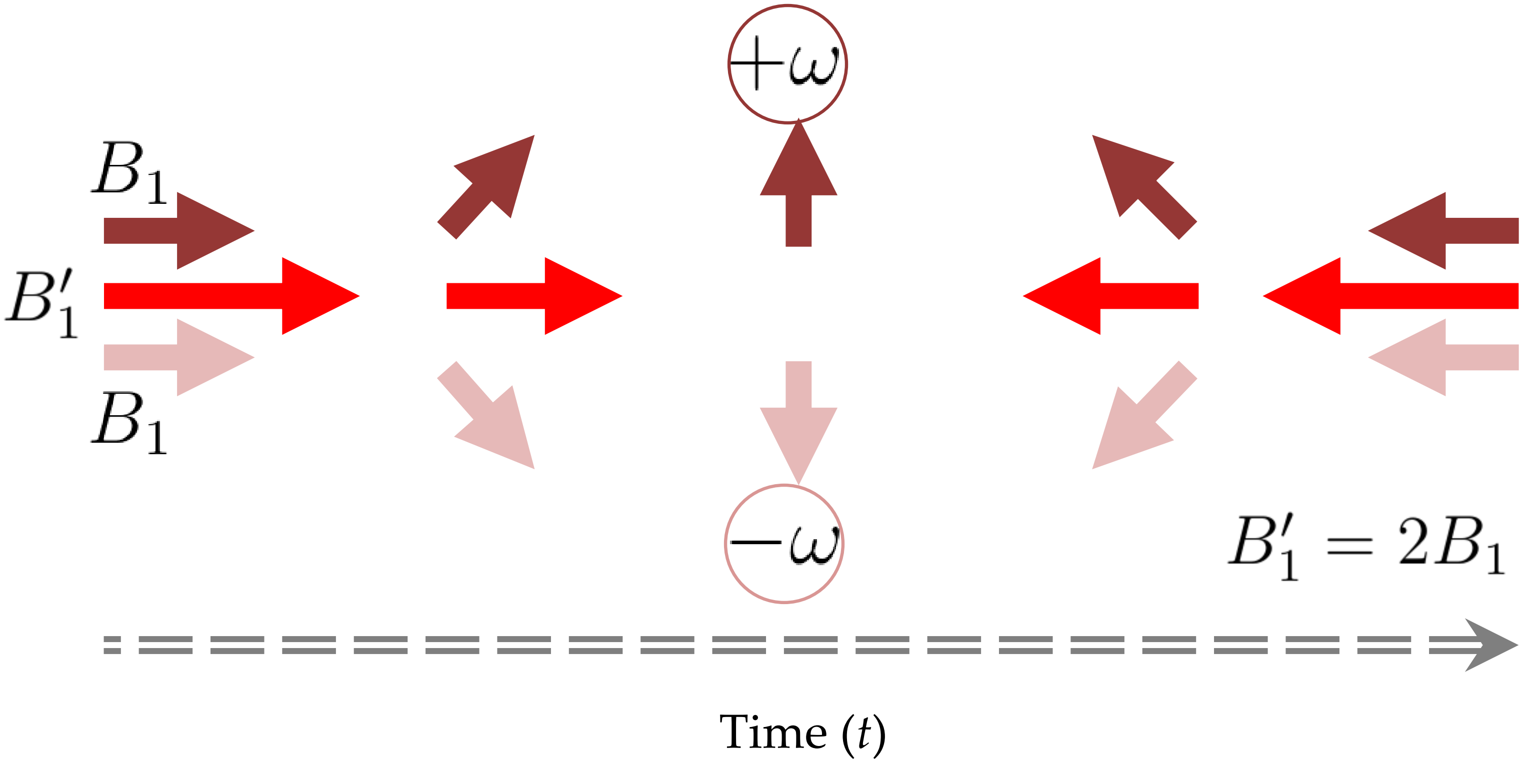

Magnetic Resonance (MR)

– In the high-field regime ($B_0 >> B_1$), use a rotating-wave approximation (RWA)

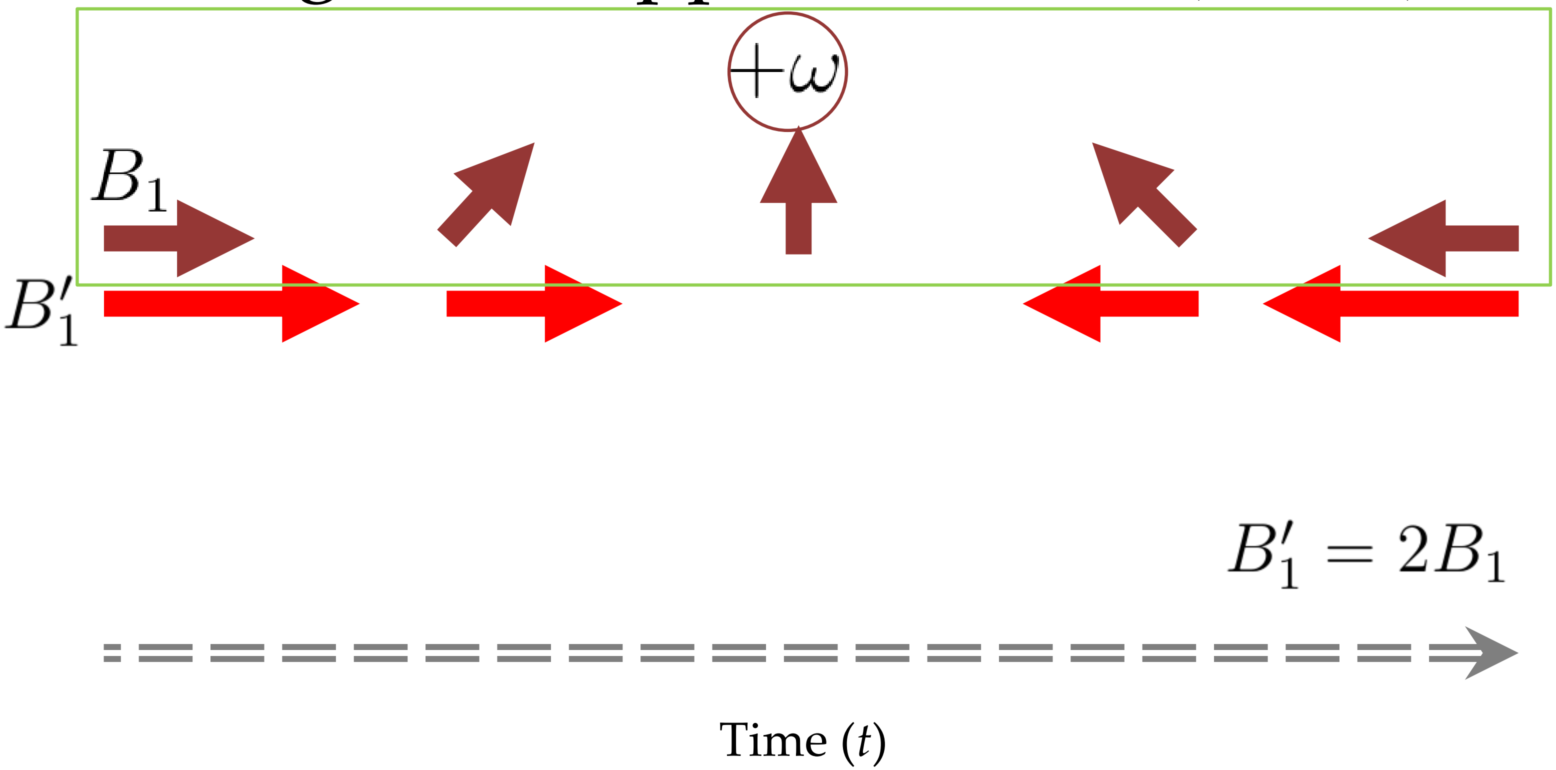

Magnetic Resonance (MR)

– The magnetic fields and spin state can be visualized using a Bloch-sphere picture

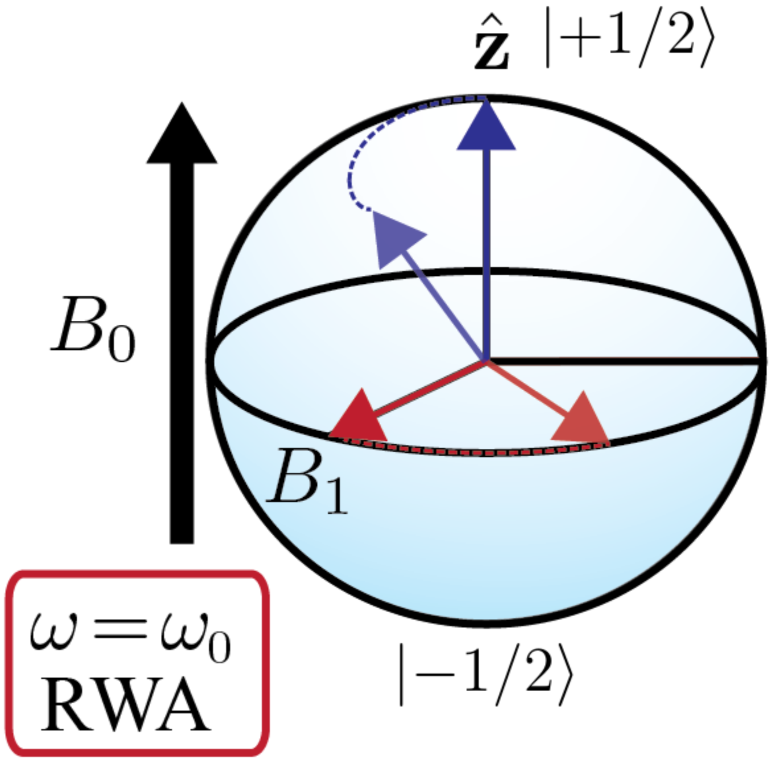

Magnetic Resonance (MR)

– Considering a rotating-frame Bloch sphere (RFBS) elucidates spin dynamics

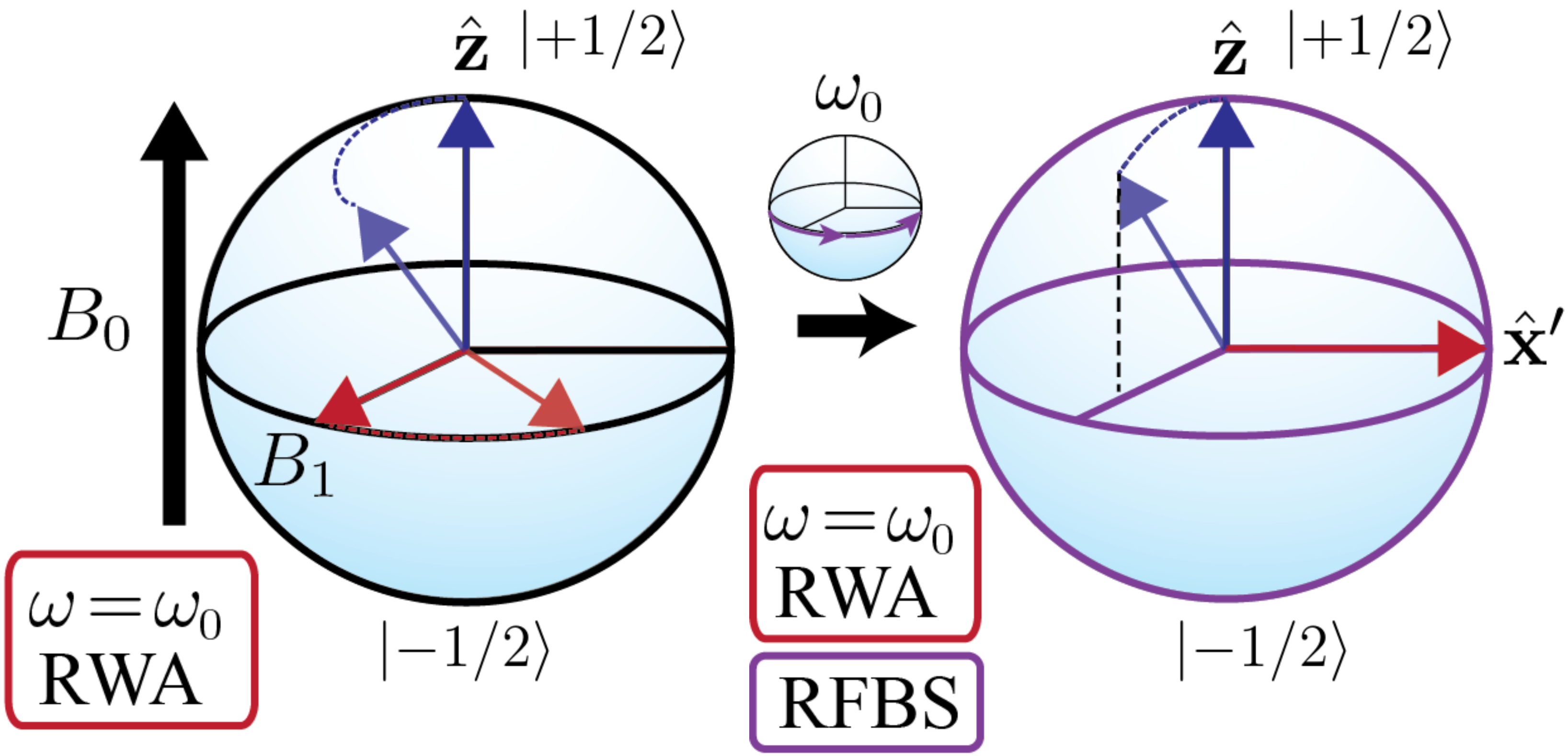

Magnetic Resonance (MR)

– In this way, the dynamics are also well visualized for a non-resonant pulse

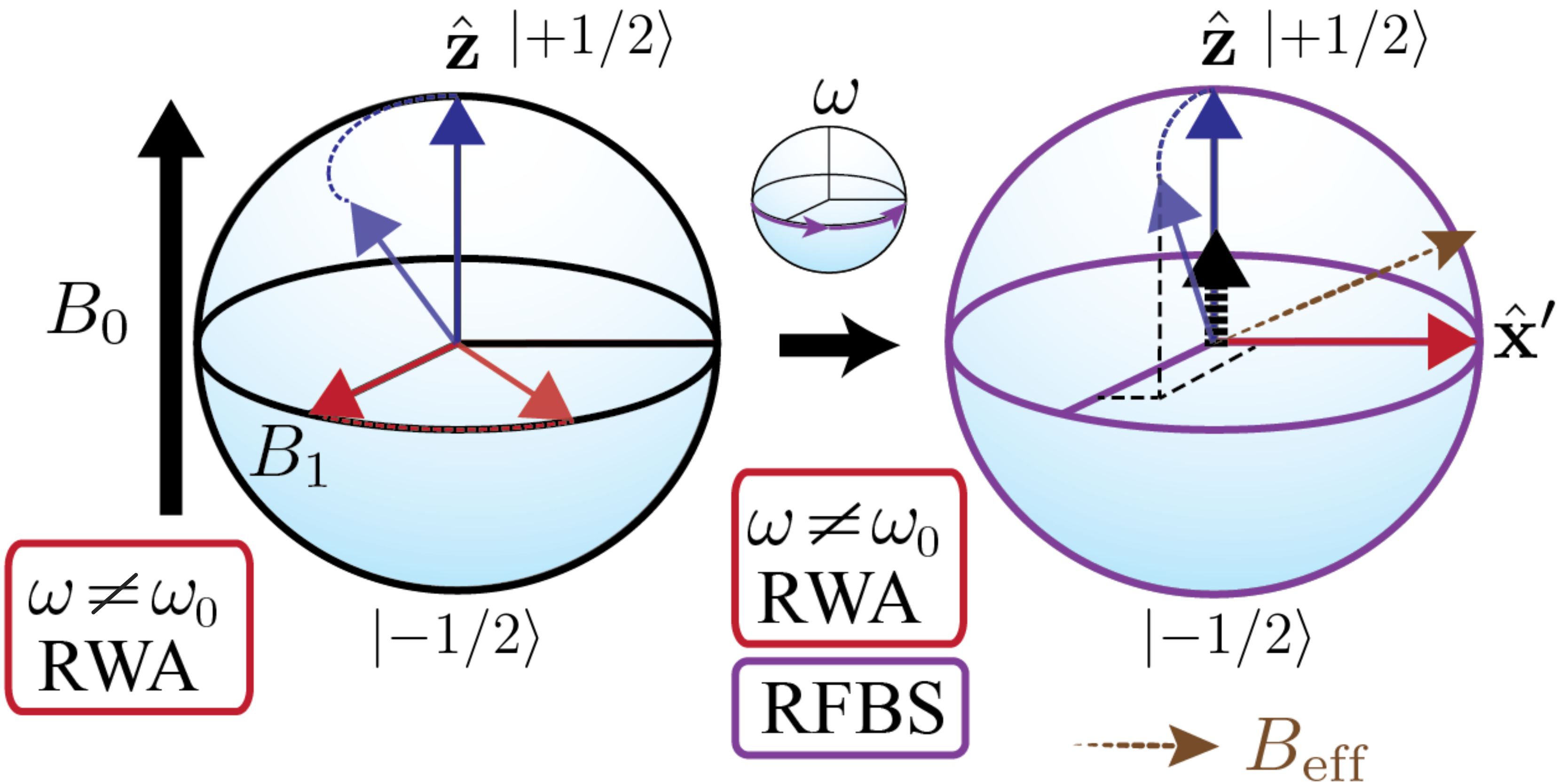

Magnetic Resonance (MR)

– This nutation about B_{eff} is well-described quantitatively in a Rabi oscillation

$$\Omega = \gamma B_1$$

$$\Omega_R = \sqrt{\Omega^2 + (\omega - \omega_0)^2}$$

$$(= \gamma B_{\text{eff}})$$

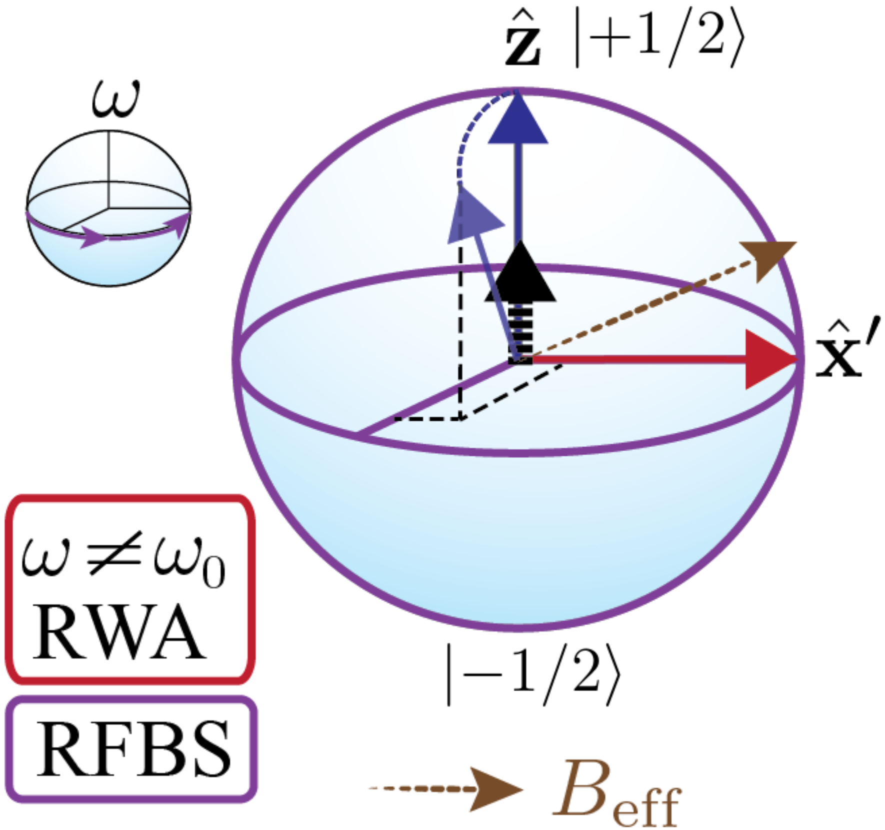

Nuclear MR (NMR)

– NMR samples have many spins, thermally polarized, totaling a net magnetization **M**

$$P_0 = P_\uparrow - P_\downarrow$$

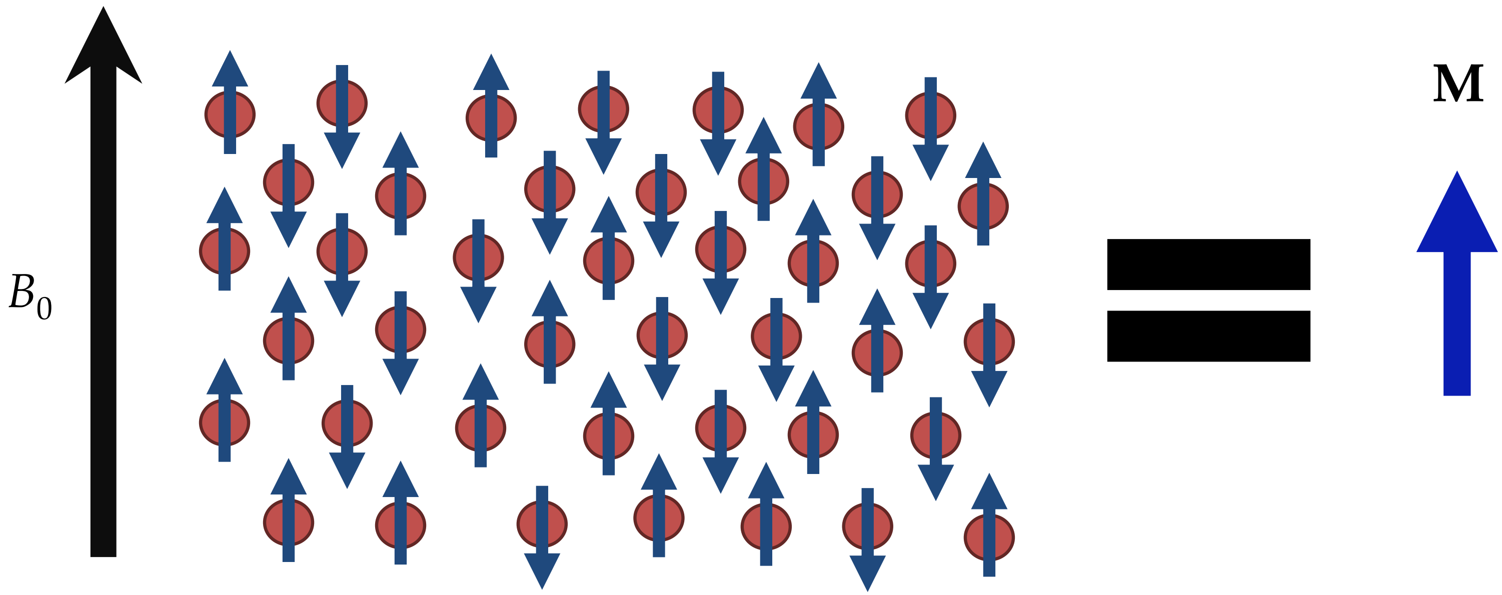

Nuclear MR (NMR)

- **M** is (conventionally) a pseudo-pure spin state, and only mimics a single spin state

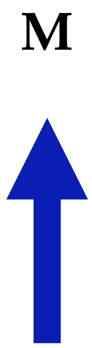

Nuclear MR (NMR)

– However, as a proper sum of its spin constituents, **M** obeys the same dynamics

$$P_{\downarrow} = \frac{\Omega^2}{\Omega_R^2} \sin^2\left(\frac{\Omega_R}{2} t\right)$$

M

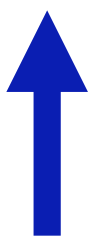

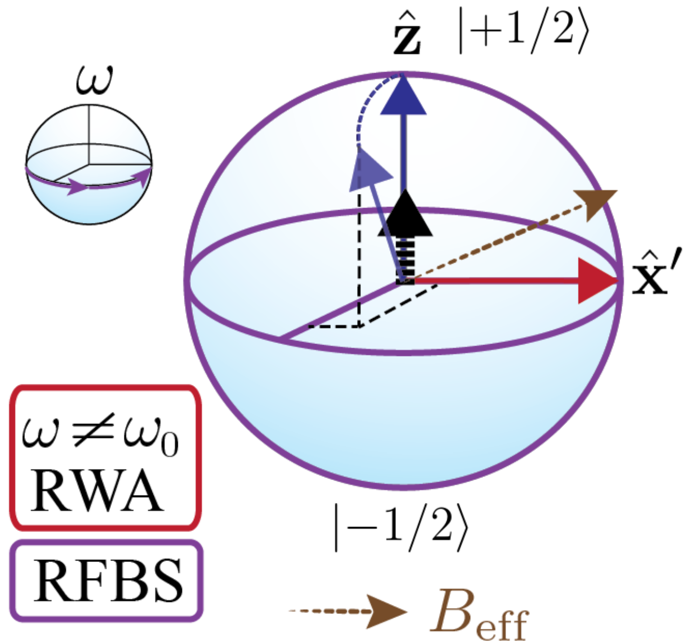

Nuclear MR (NMR)

– A typical, pulsed-NMR experiment relies on the function of a single coil

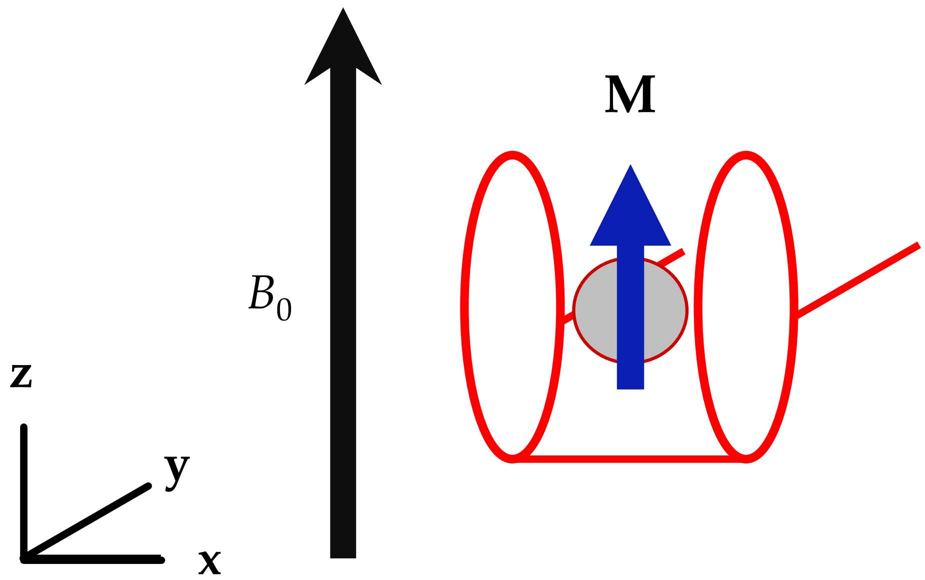

Nuclear MR (NMR)

– The coil is first pulsed at the resonance frequency, causing a Rabi oscillation of **M**

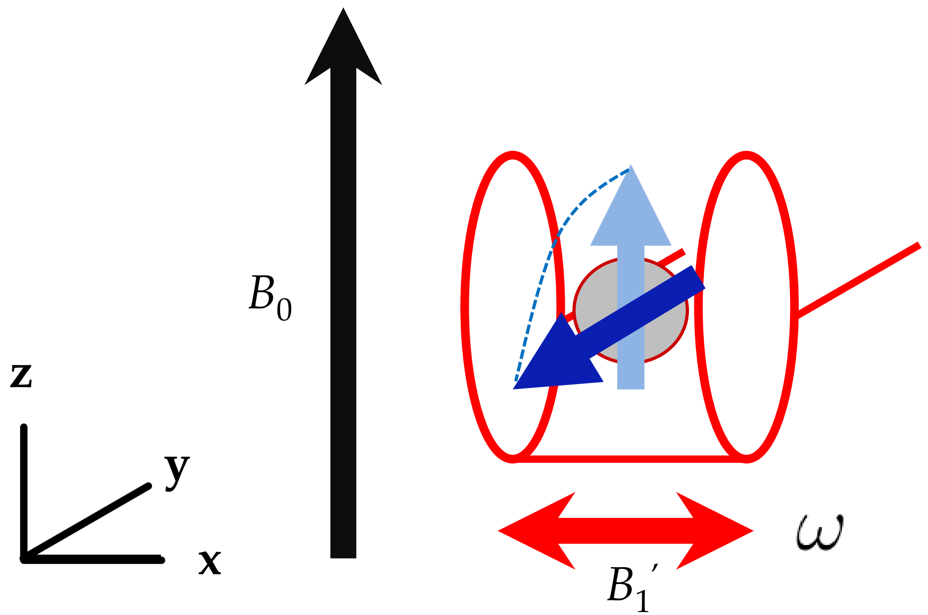

Result of a 90°, or $\pi/2$, flip angle

Nuclear MR (NMR)

– **M** is torqued about B_0, inducing an EMF, and generates a free induction decay (FID)

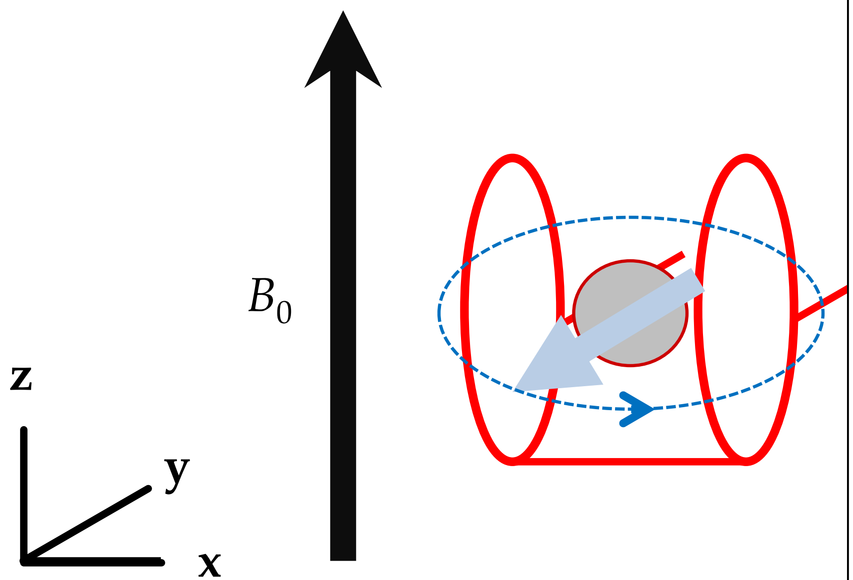

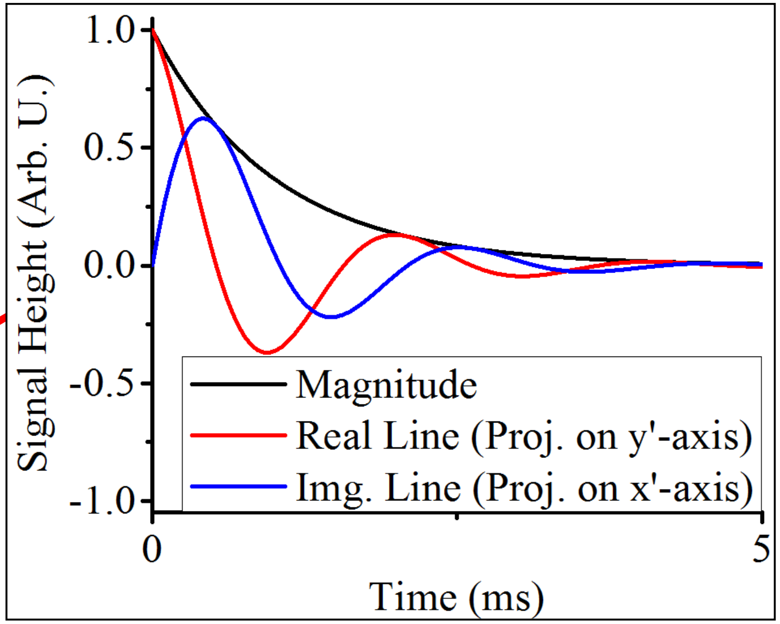

Nuclear MR (NMR)

- Decay results from dephasing of spins due to local environment (local field)

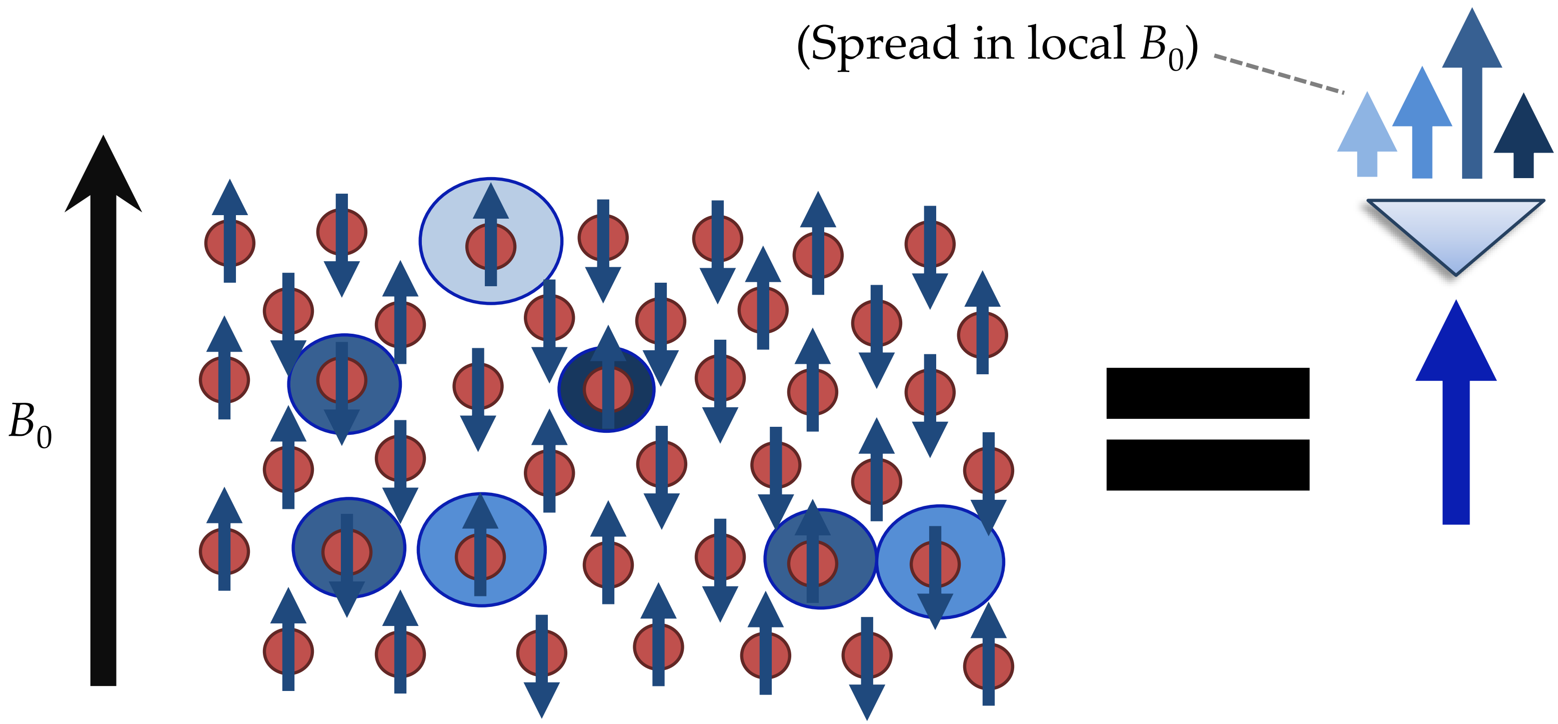

Nuclear MR (NMR)

– The decay results from dephasing of spins due to local environment (local field)

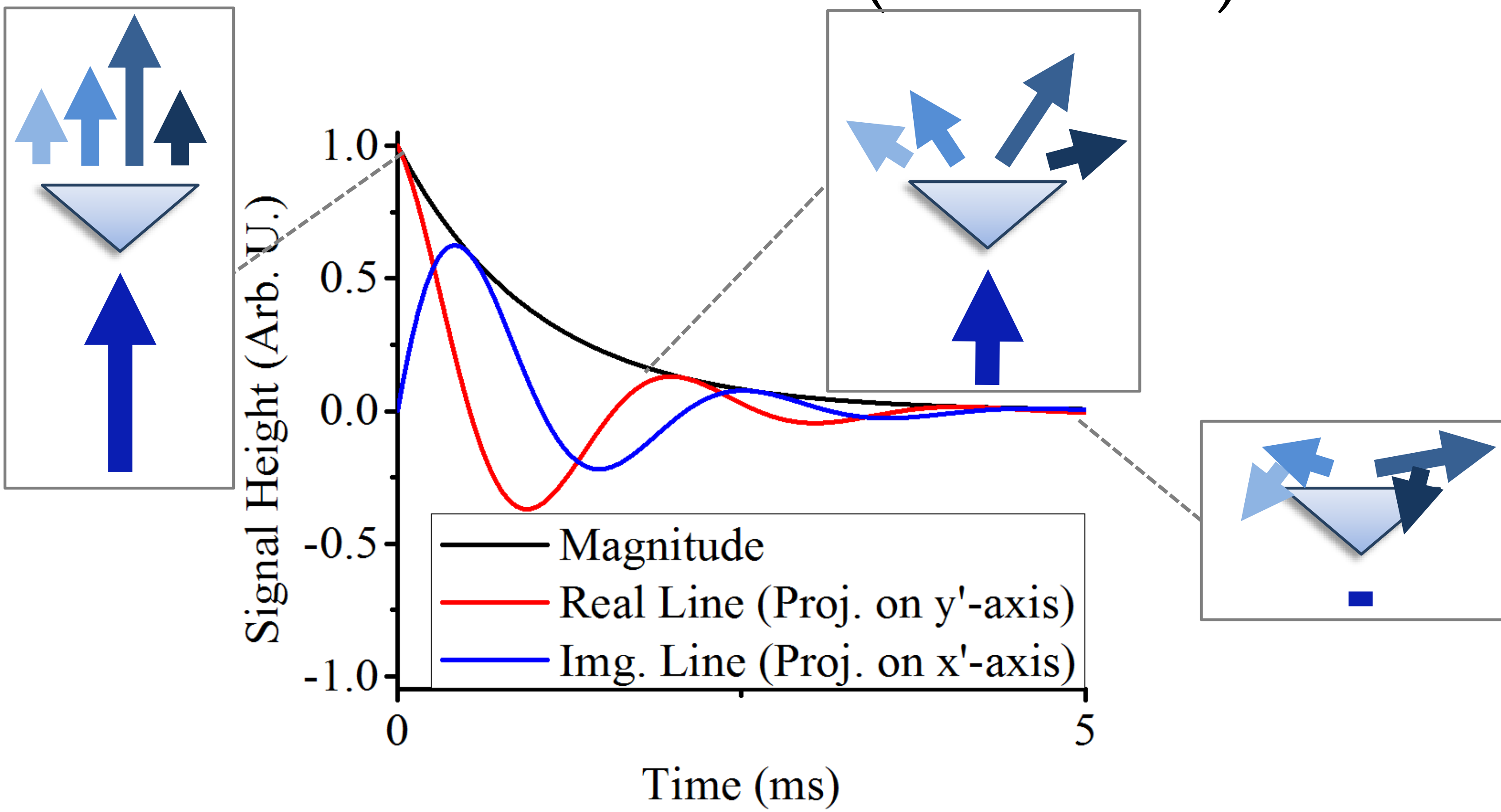

Nuclear MR (NMR)

– For some systems, the FID can described by characteristic relaxation time T_2

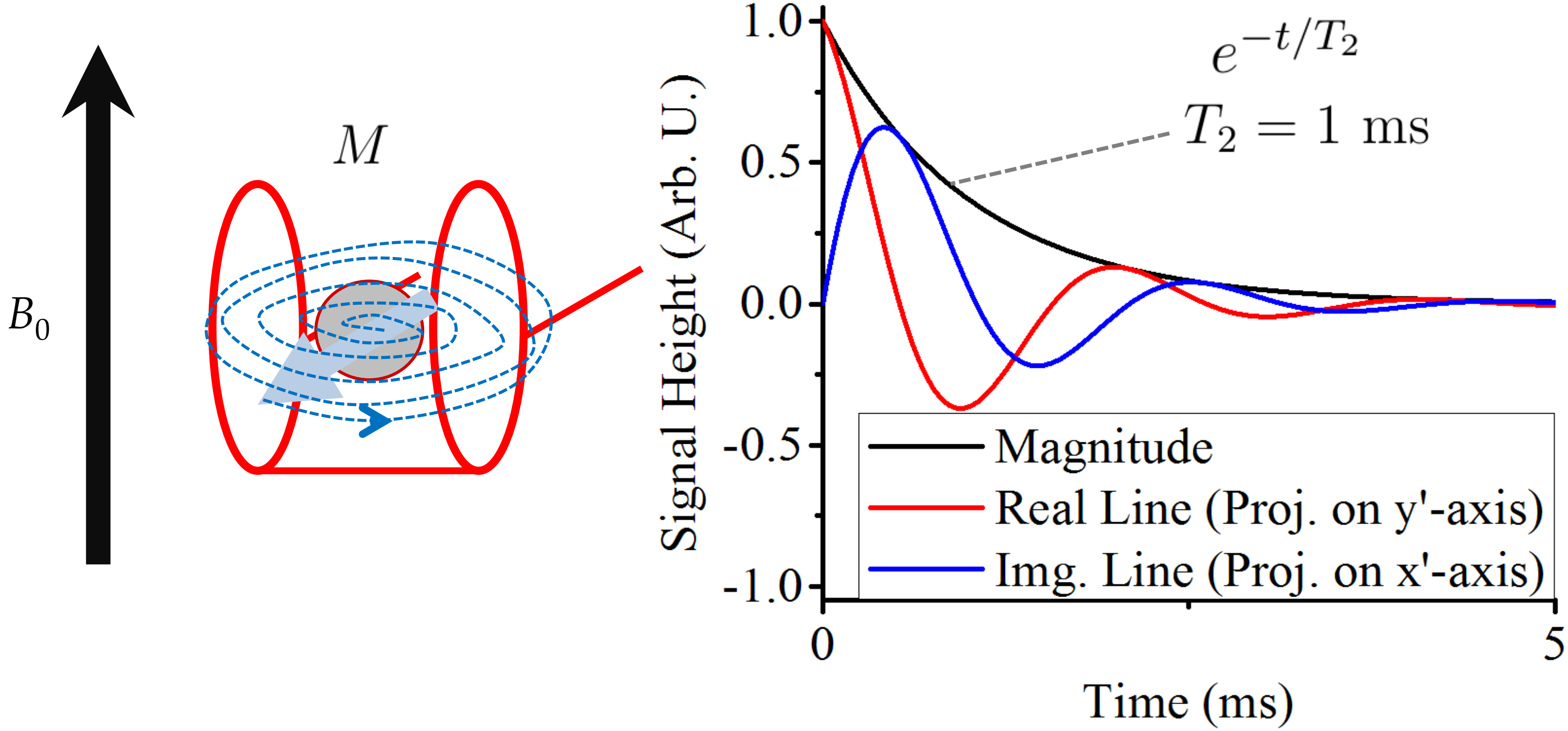

Nuclear MR (NMR)

– A Fourier transform (FFT) of the FID gives a mapping to local field distributions

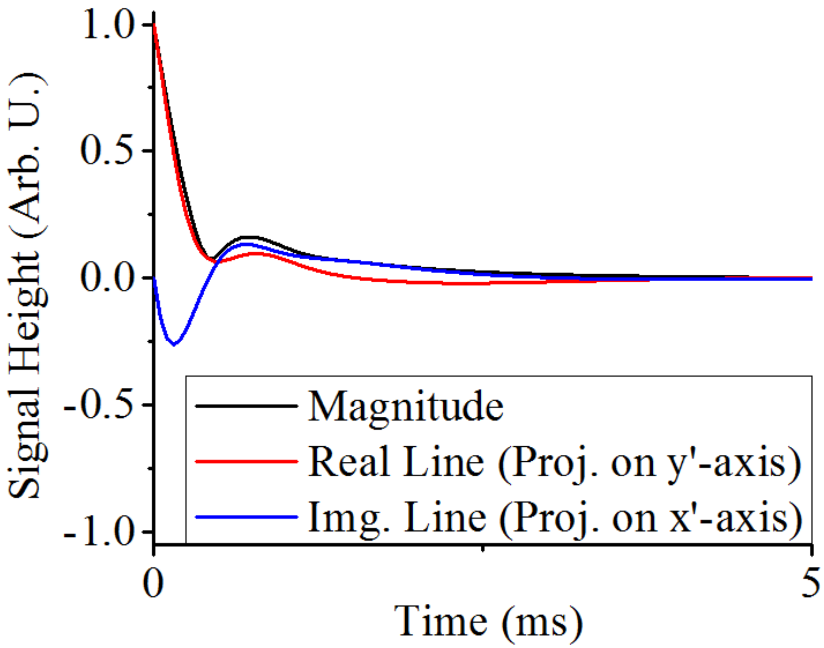

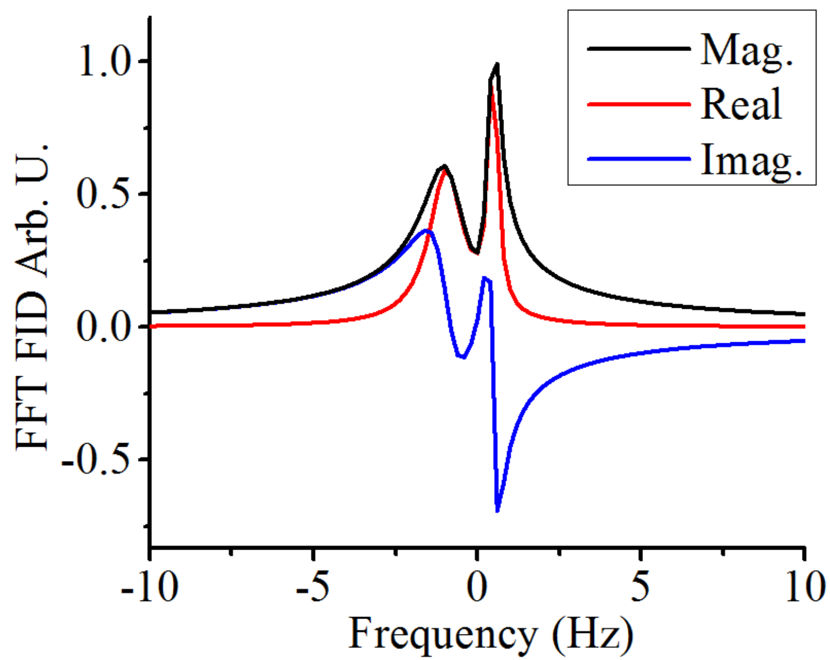

Nuclear MR (NMR)

– After dephasing, spins return to thermal equilibrium with characteristic time T_1

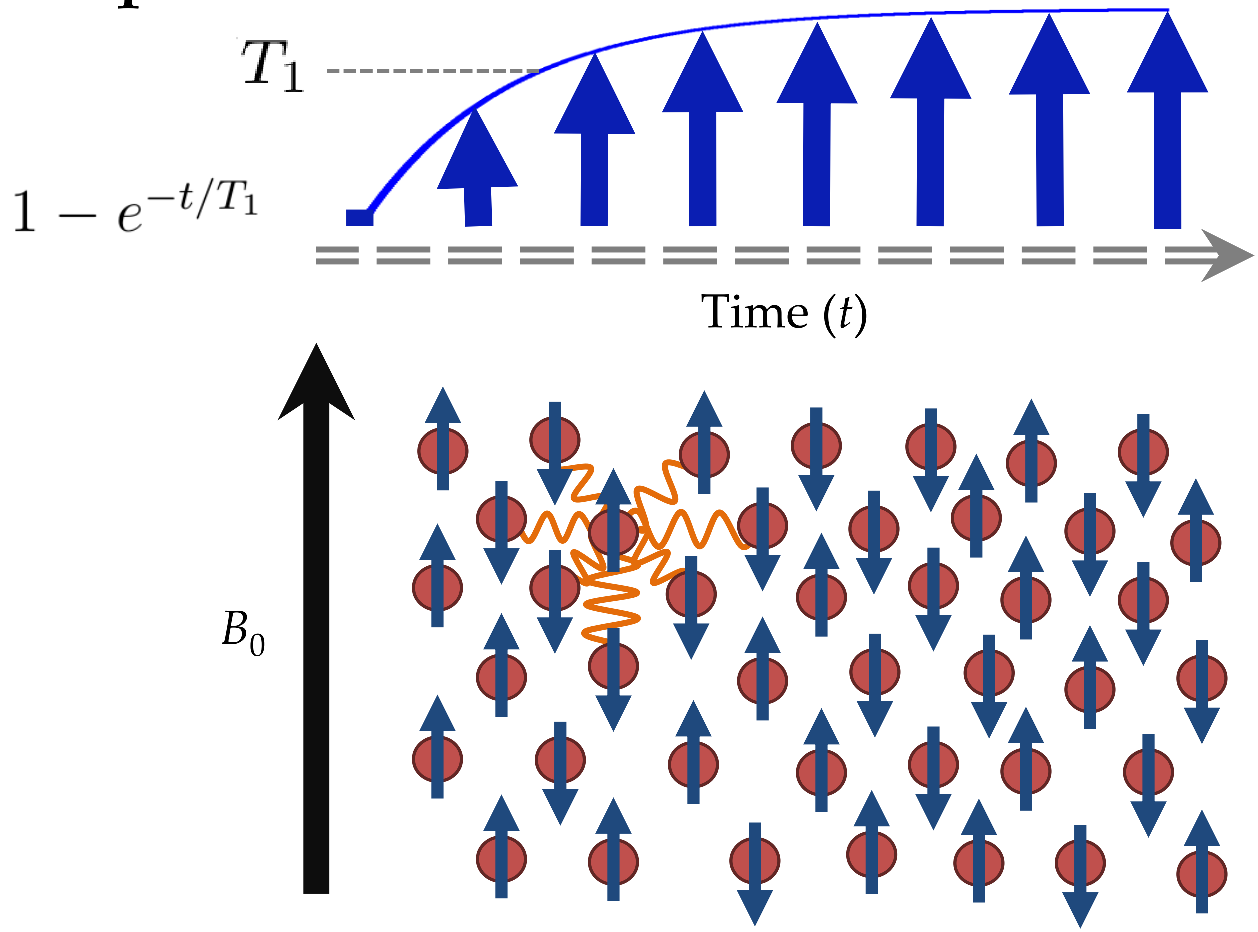

Hyperpolarization

– Spin-exchange optical pumping (SEOP) increases nuclear polarization by five orders of magnitude

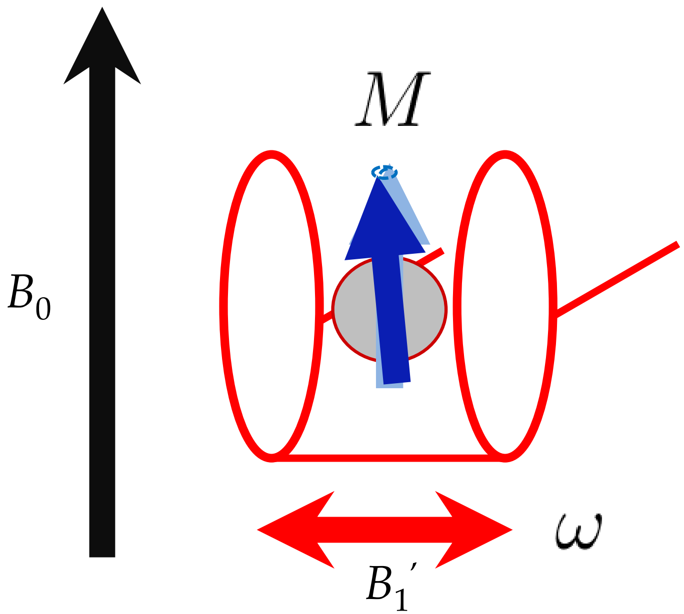

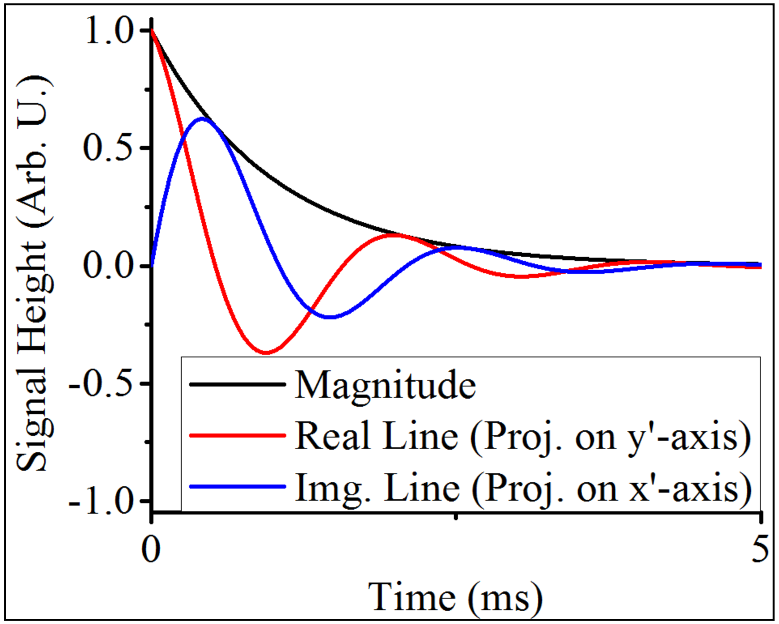

Hyperpolarization

– This boost in signal allows for T_1 experiments to be run from the 'top down'

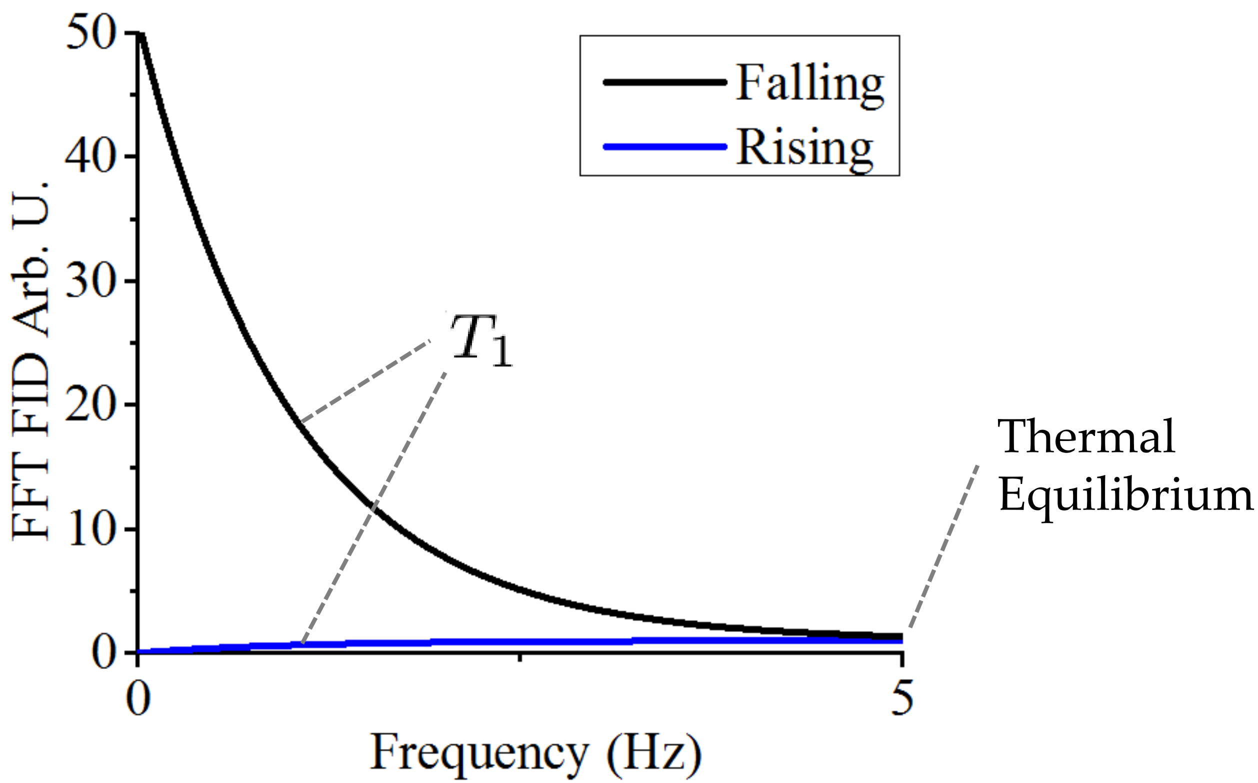

Optical Pumping

– Optically pumped alkali metal vapor approaches 100% atomic polarization

Ignoring Hyperfine

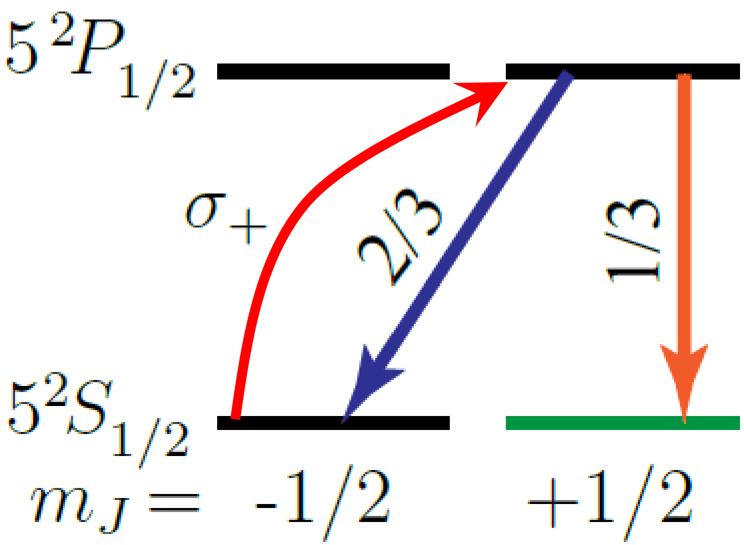

Average # of photons: 3/2

With buffer gas (N_2)

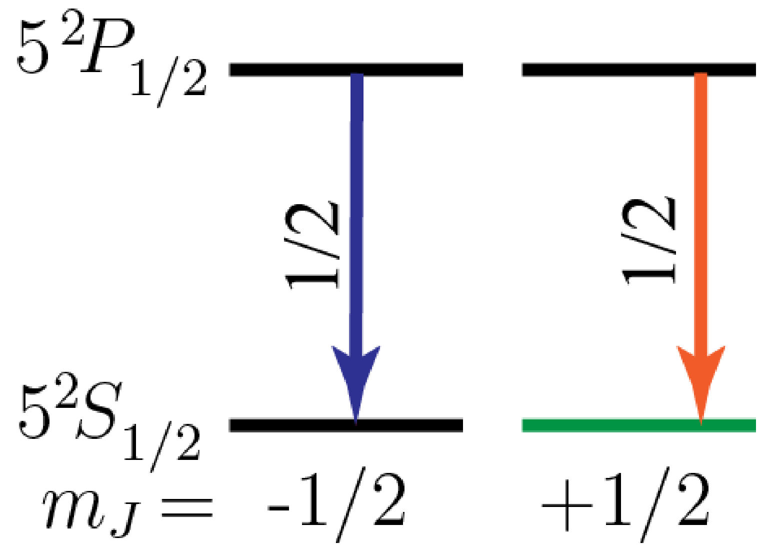

Average # of photons: 1

Optical Pumping

– Calculate single photons being absorbed by an atom, in various conditions

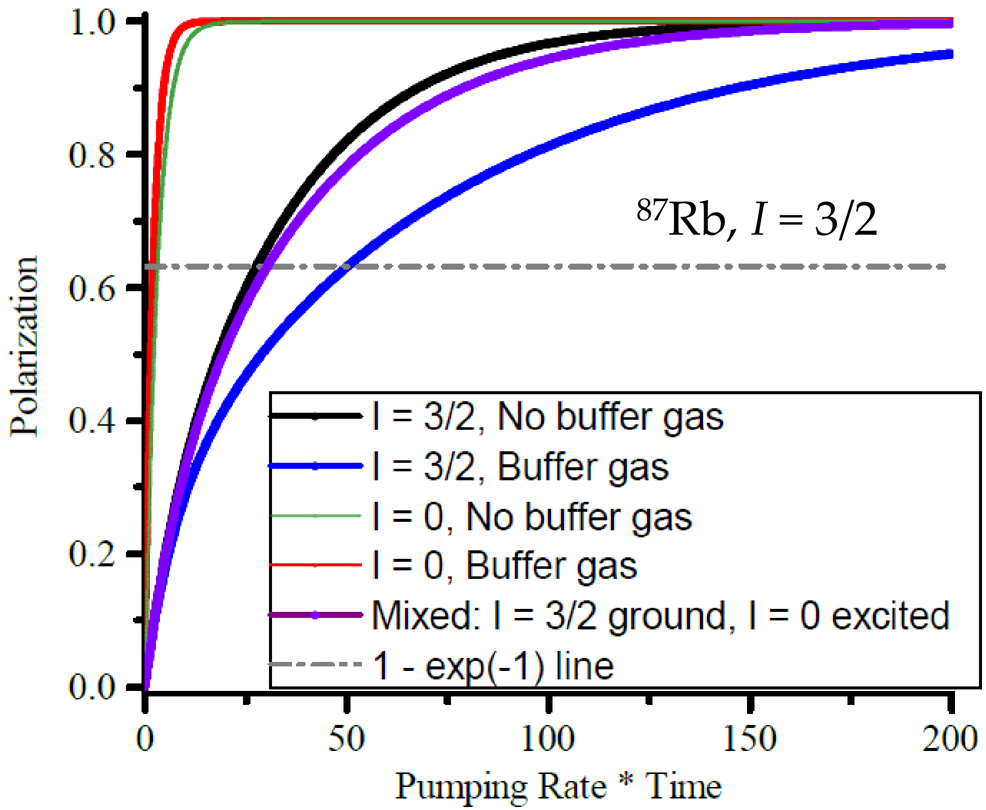

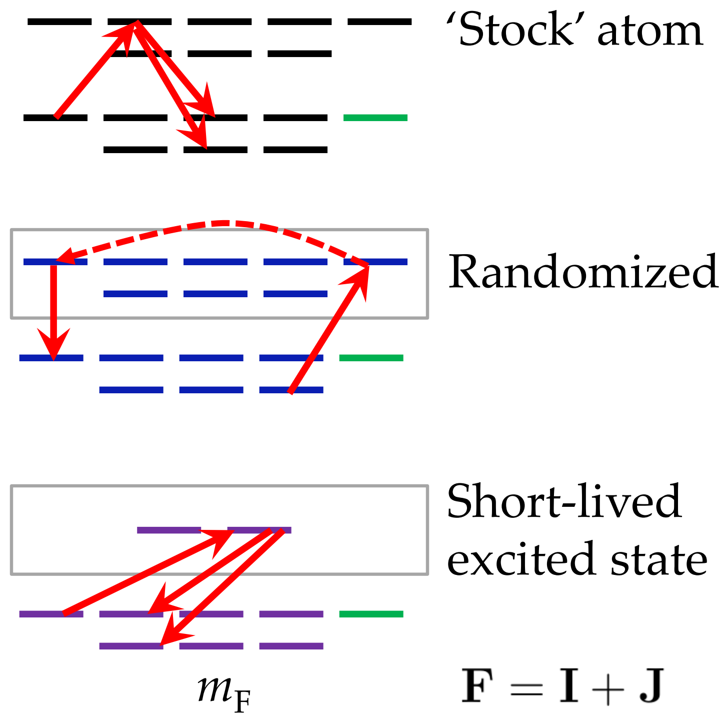

Average # of photons: 41.66

^{85}Rb, I = 5/2 Average # of photons: 115.4

SEOP

– A highly polarized atomic spin-bath contacts with a nuclear spin-bath

$$H = A\mathbf{I}\cdot\mathbf{S} + \gamma\mathbf{S}\cdot\mathbf{N} + \alpha\mathbf{K}\cdot\mathbf{S}$$

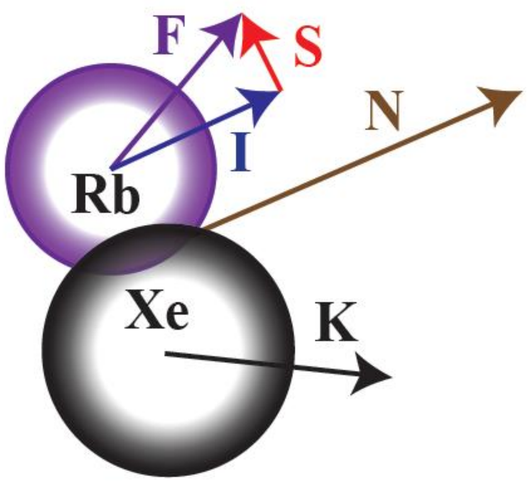

T_1 : Solid ^{129}Xe Relaxation

Methods: Solid ^{129}Xe Relaxation

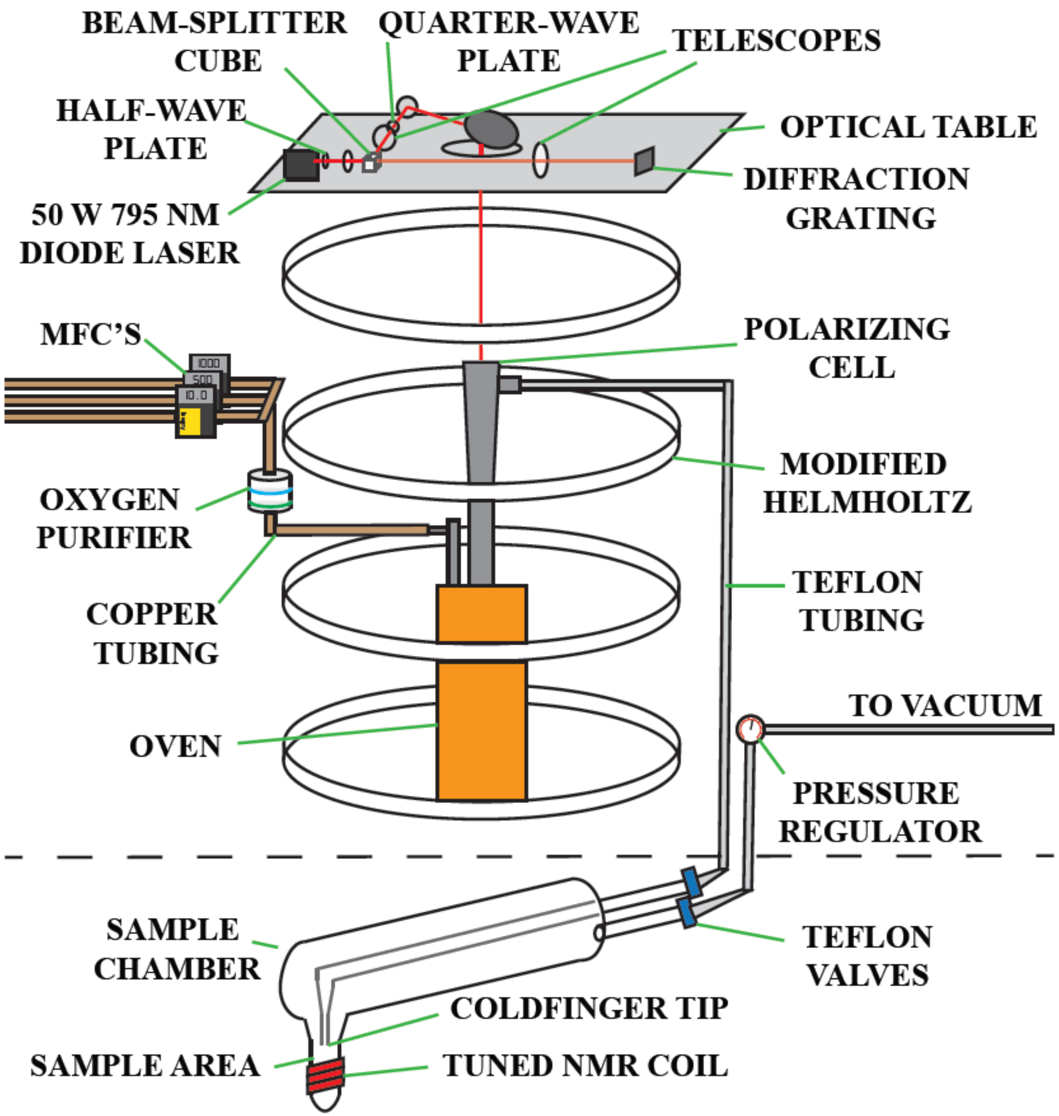

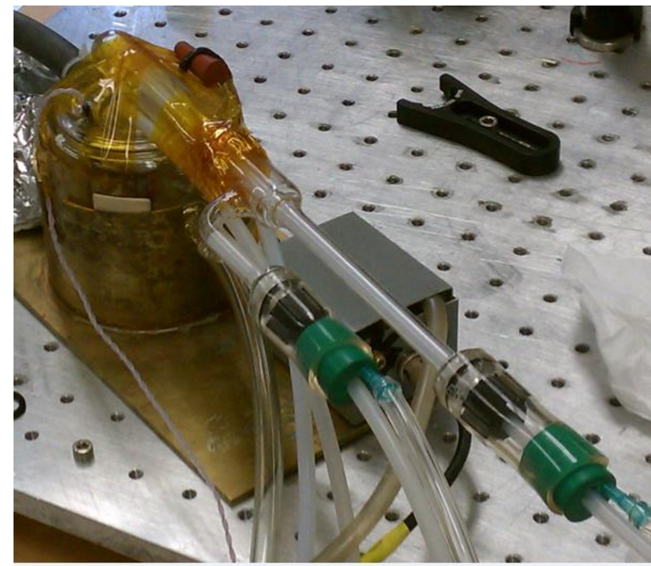

Methods: Solid ^{129}Xe Relaxation

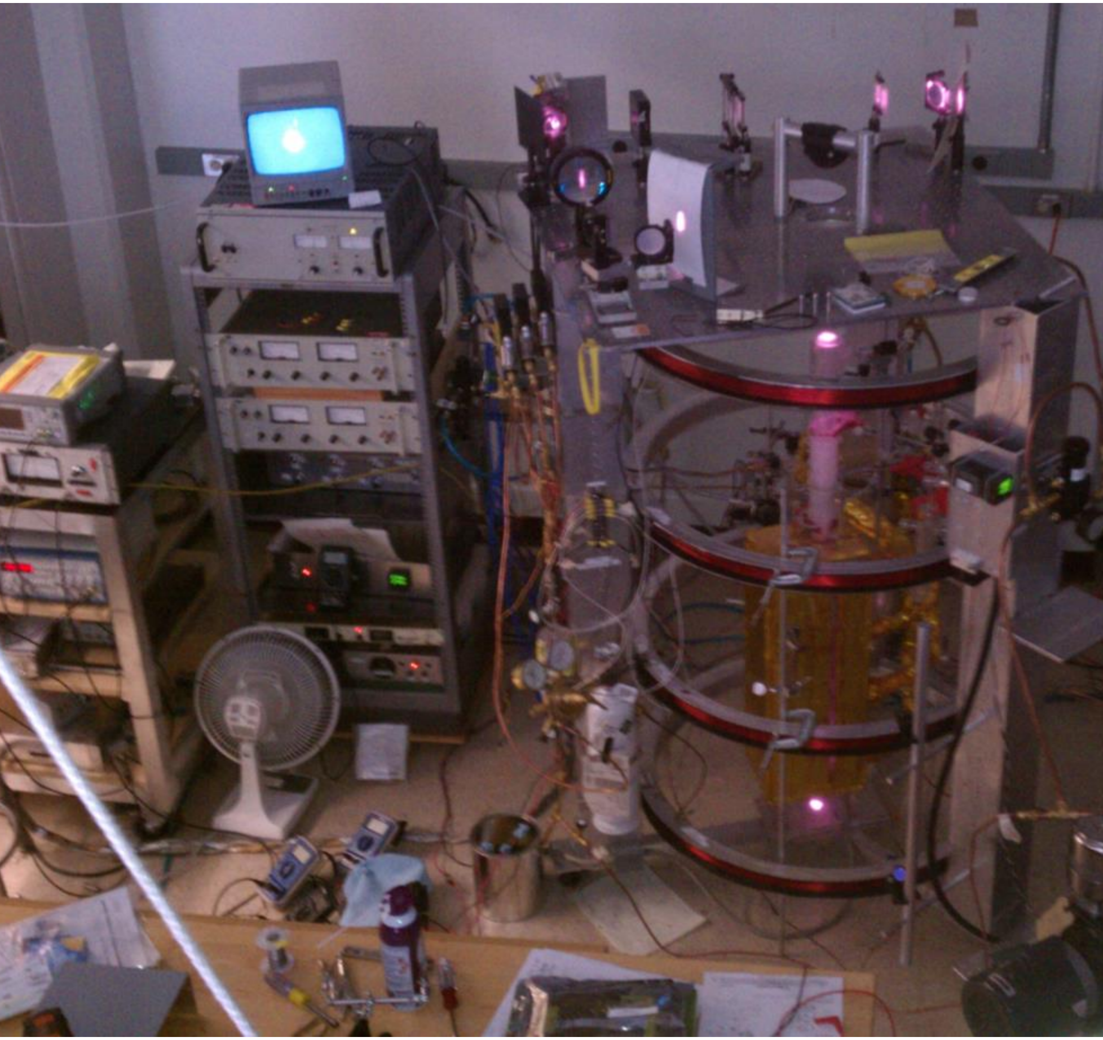

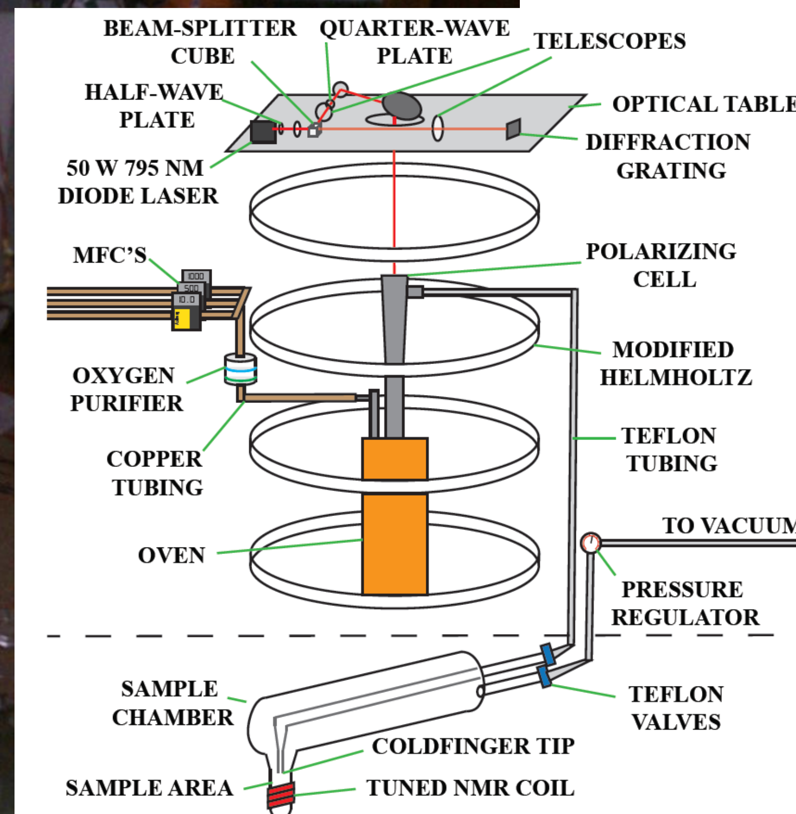

Methods: Solid ^{129}Xe Relaxation

– Trickle-freeze hyperpolarized xenon into sample chamber (Snow) held at 2 Tesla

– Set temperature of sample and perform T_1 experiment, with extremely small flip angles (approx. 1-8°)

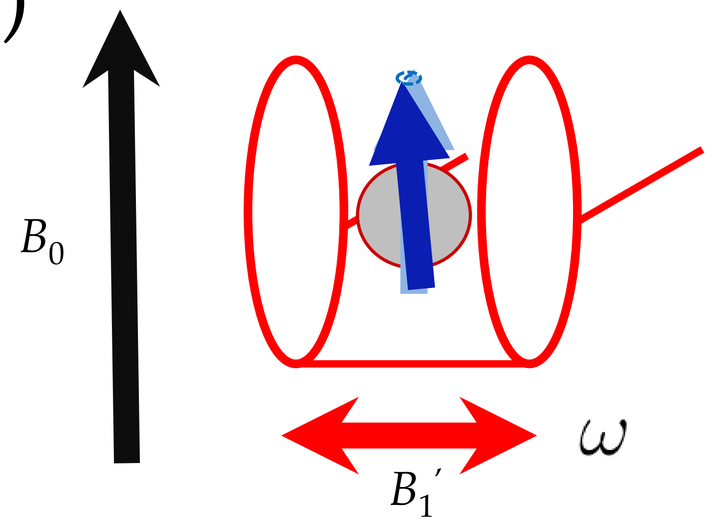

Methods: Solid ^{129}Xe Relaxation

– Able to take snow through liquid phase, and refreeze at 77 K (Ice)

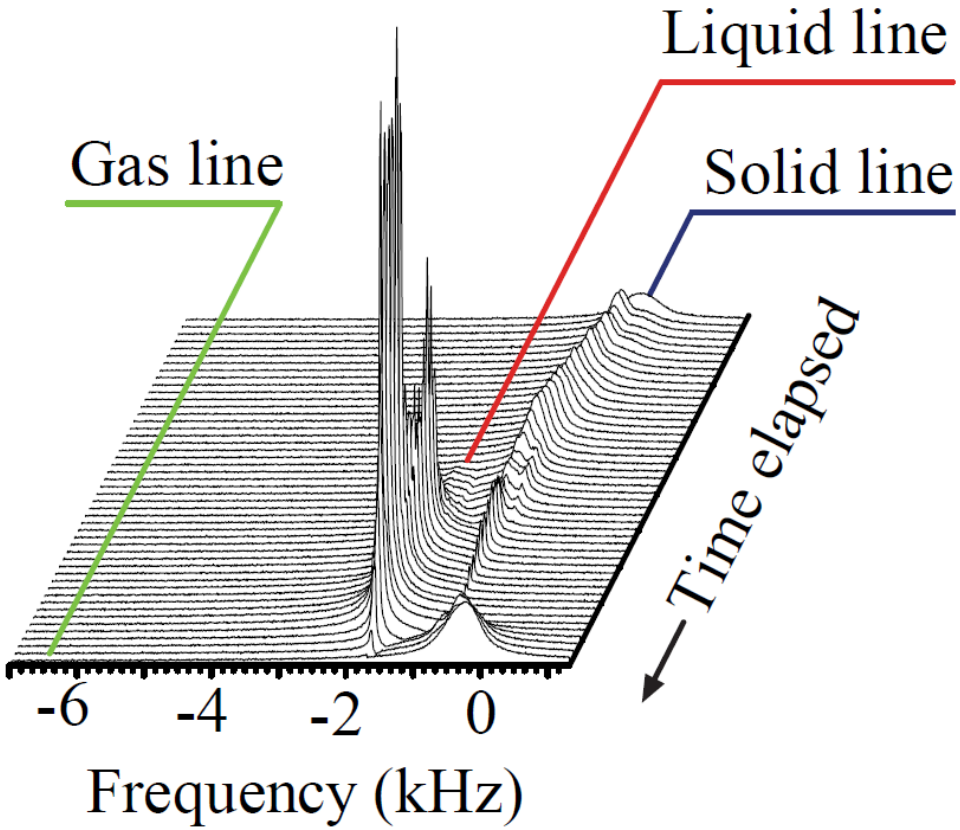

Results: Solid ^{129}Xe Relaxation

– See a substantial difference between ice and snow relaxation times at 77 K

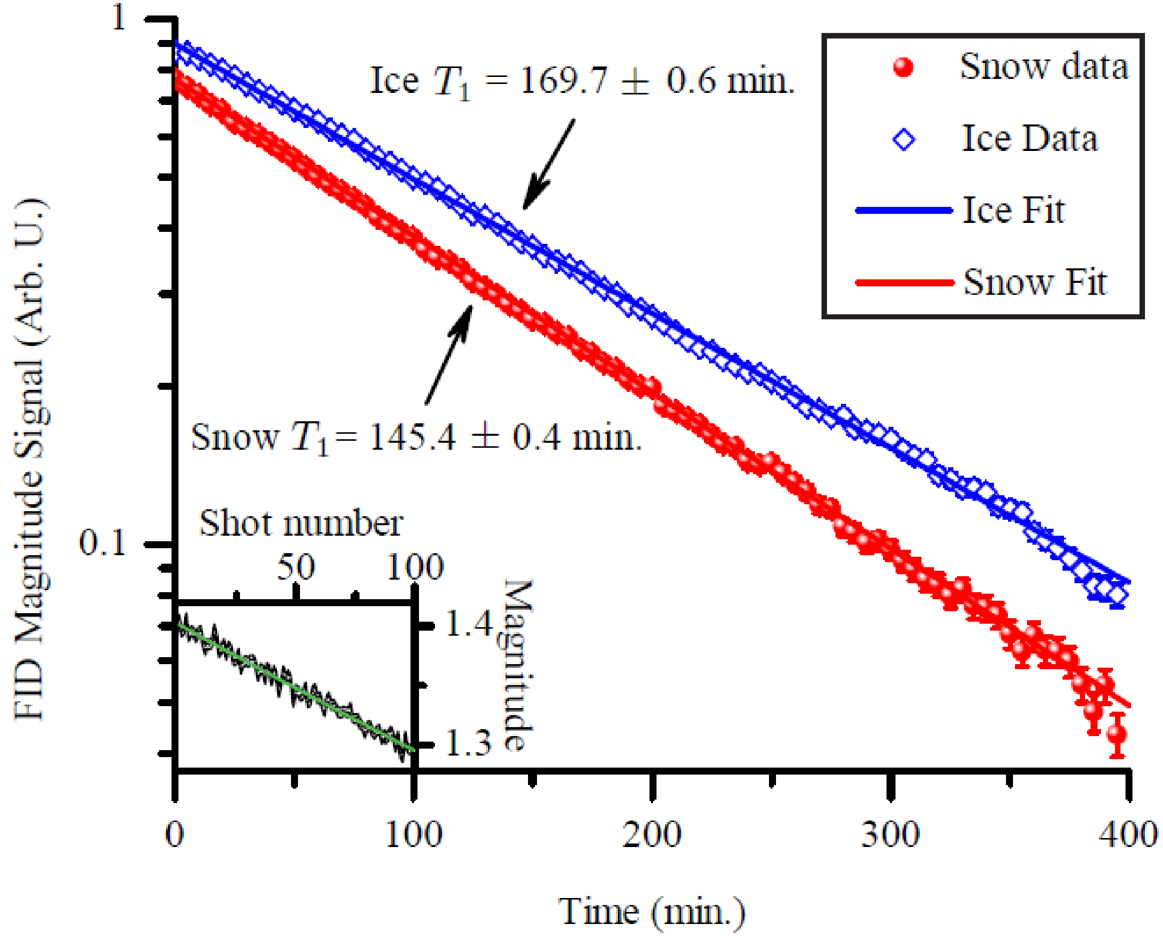

Results: Solid ^{129}Xe Relaxation

– Difference is reproducible across many set-ups

77 K

	T_1 (min.)	Probe	Flip Angle	Buffer Gas
Ice	169.93 ± 0.25	Tank	N/A	Yes
	168.16 ± 0.16	Tank	N/A	No
	165.14 ± 0.70	Tank	N/A	Yes
	168.7 ± 1.0	Tank	N/A	Yes
	173.6 ± 1.5	Tank	N/A	Yes
	171.44 ± 0.32	Flat	$2.67^\circ \pm 0.19^\circ$	Yes
	172.02 ± 0.31	Flat	$3.11^\circ \pm 0.30^\circ$	No
	166.55 ± 0.81	Flat	$3.02^\circ \pm 0.07^\circ$	No
	167.30 ± 0.33	Flat	$3.31^\circ \pm 0.32^\circ$	Yes
Ice Average	169.2 ± 1.2			

Snow	150.79 ± 0.43	Tank	N/A	No
	148.47 ± 0.28	Tank	N/A	Yes
	150.80 ± 0.25	Tank	N/A	Yes
	148.61 ± 0.42	Flat	$8.96^\circ \pm 0.05^\circ$	No
	149.30 ± 0.40	Flat	$6.27^\circ \pm 0.07^\circ$	Yes
	149.80 ± 0.40	Flat	$6.91^\circ \pm 0.14^\circ$	Yes
	150.19 ± 0.37	Flat	$6.91^\circ \pm 0.14^\circ$	Yes
	151.02 ± 0.51	Flat	$4.67^\circ \pm 0.22^\circ$	No
Snow Average	149.87 ± 0.54			

Results: Solid ^{129}Xe Relaxation

Snow-oxygen introduction at 77 K

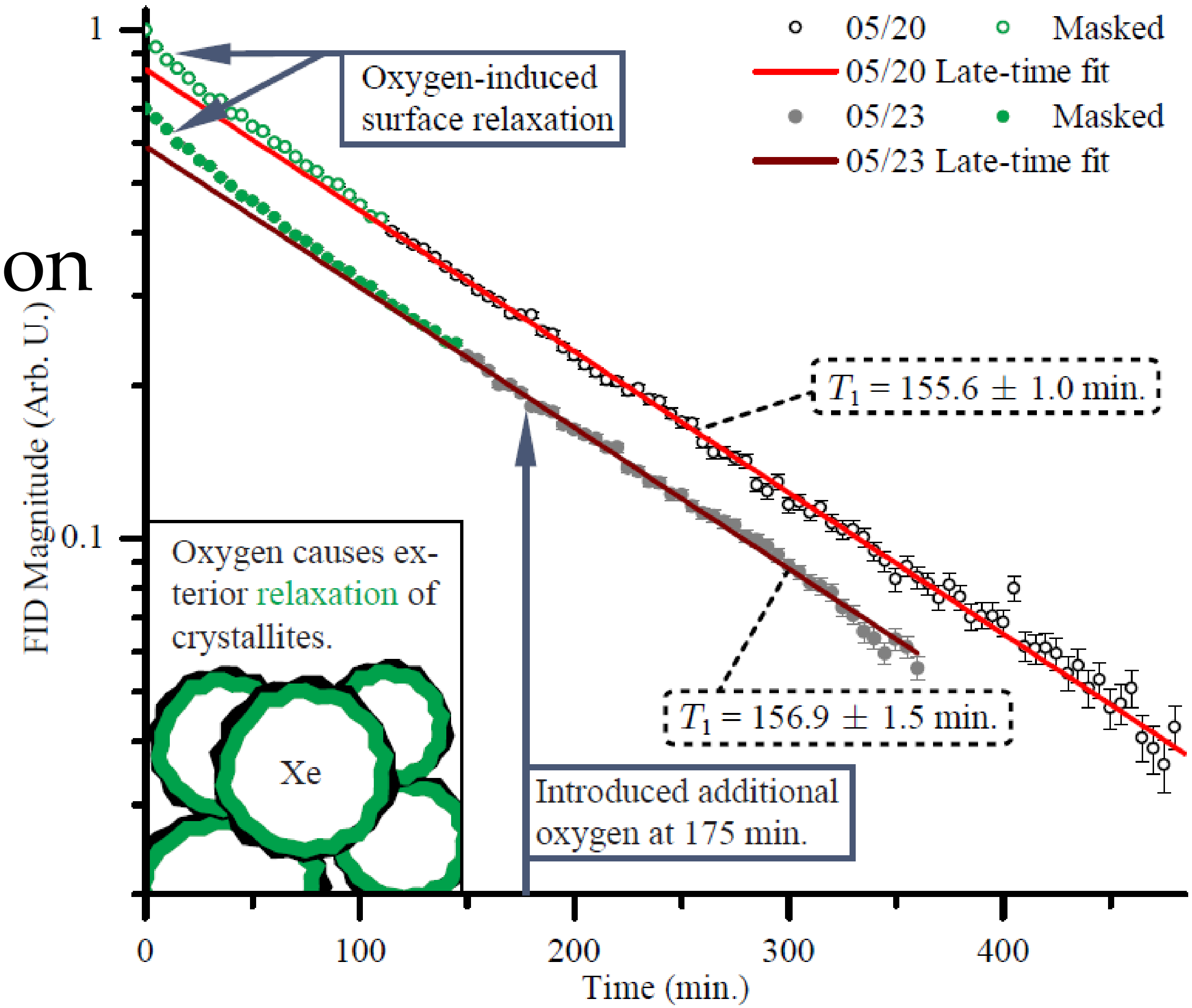

Results: Solid ^{129}Xe Relaxation

- Intrinsic difference in ^{129}Xe T_1 between bulk snow and ice

- Theory predicts no difference between polycrystalline and single crystal ^{129}Xe T_1

- Initial results at 77 K indicate ice T_1 is *longer* than theory suggests

Results: Solid ^{129}Xe Relaxation

Ice

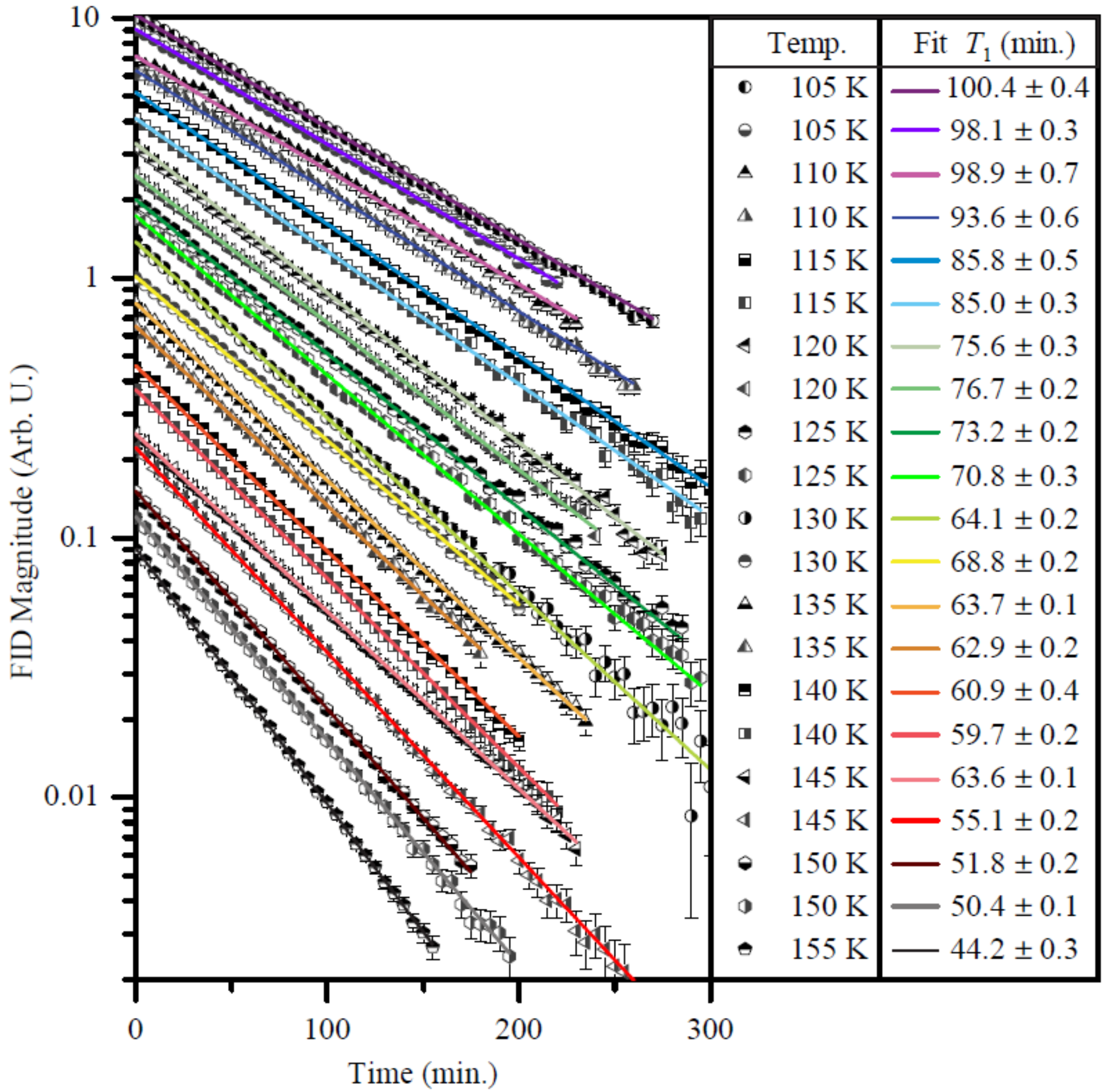

Results: Solid ^{129}Xe Relaxation

Ice

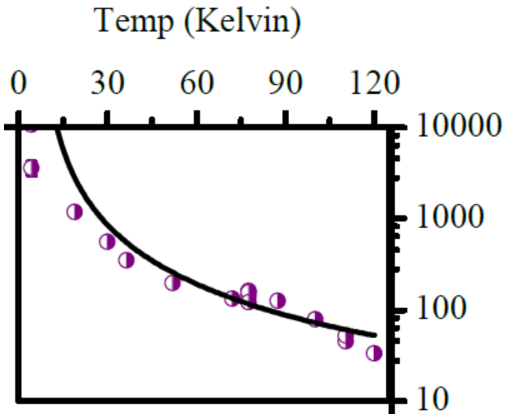

Low-temperature diverges from theory

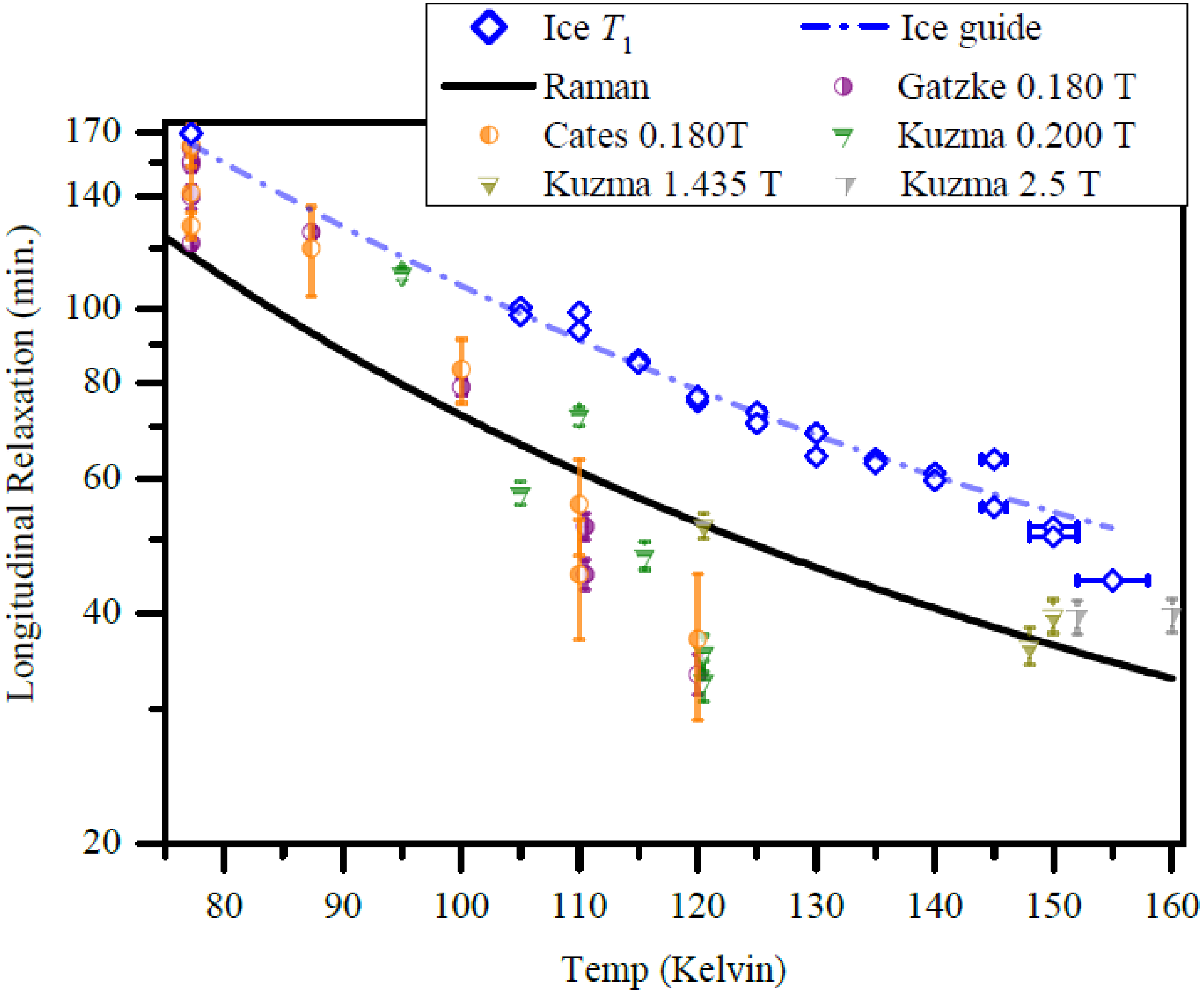

Theory: Solid ^{129}Xe Relaxation

– Spin-rotation is dominate gas mechanism

$$^{129}\text{Xe-Xe}$$

Theory: Solid ^{129}Xe Relaxation

– Spin-rotation is dominate gas mechanism

THEORY OF QUADRUPOLAR NUCLEAR SPIN-LATTICE RELAXATION

by J. VAN KRANENDONK

PHYSICAL REVIEW B VOLUME 59, NUMBER 13 1 APRIL 1999-I

^{129}Xe spin relaxation in frozen xenon

R. J. Fitzgerald,* M. Gatzke,† David C. Fox,‡ G. D. Cates, and W. Happer
Department of Physics, Princeton University, Princeton, New Jersey 08544
(Received 2 September 1998)

VOLUME 18, NUMBER 17 PHYSICAL REVIEW LETTERS 24 APRIL 1967

THEORY OF QUADRUPOLAR NUCLEAR SPIN-LATTICE RELAXATION DUE TO ANHARMONIC RAMAN PHONON PROCESSES

J. Van Kranendonk and M. Walker*
Department of Physics, University of Toronto, Toronto, Canada
(Received 12 January 1967, revised manuscript received 17 February 1967)

Theory: Solid ^{129}Xe Relaxation

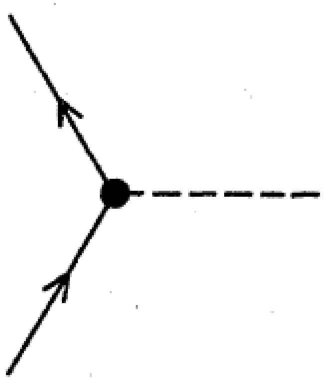

a

Direct Process (DP)
Linear temp. dependence,
Field dependent

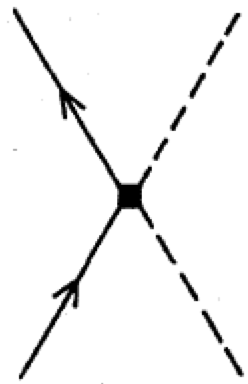

b

Harmonic Raman (1R)
Quad. temp. dependence,
Field independent

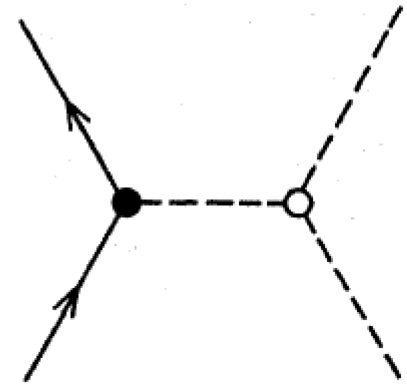

d

Anharmonic Raman (aR)
Quad. temp. dependence,
Field independent

-Van Kranendonk,
Walker, PRL, (1967)

Theory: Solid ^{129}Xe Relaxation

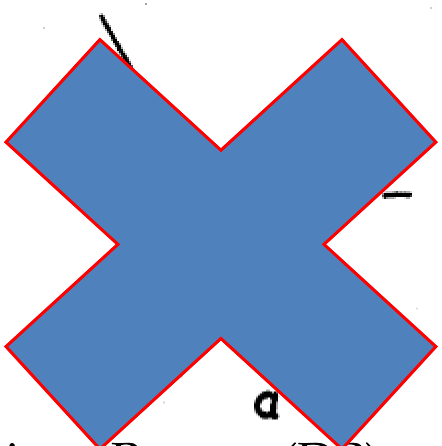

Direct Process (DP)
Linear temp. dependence,
Field dependent

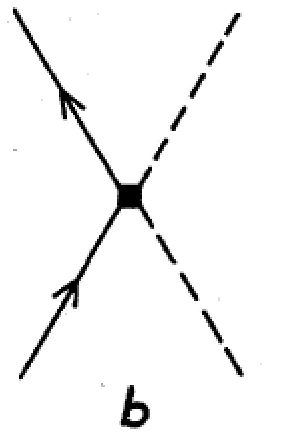

Harmonic Raman (1R)
Quad. temp. dependence,
Field independent

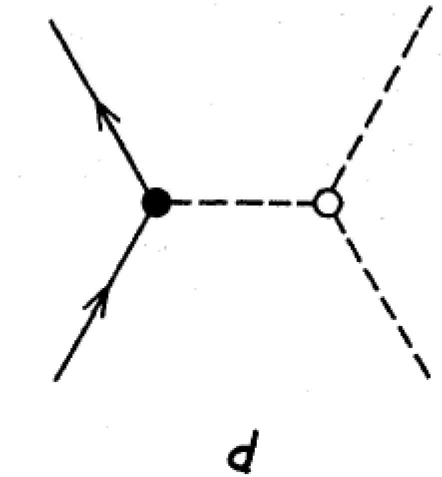

Anharmonic Raman (aR)
Quad. temp. dependence,
Field independent

Too weak/improbable

-Van Kranendonk,
Walker, PRL, (1967)

Theory: Solid ^{129}Xe Relaxation

– Direct processes less probable than two-phonon processes

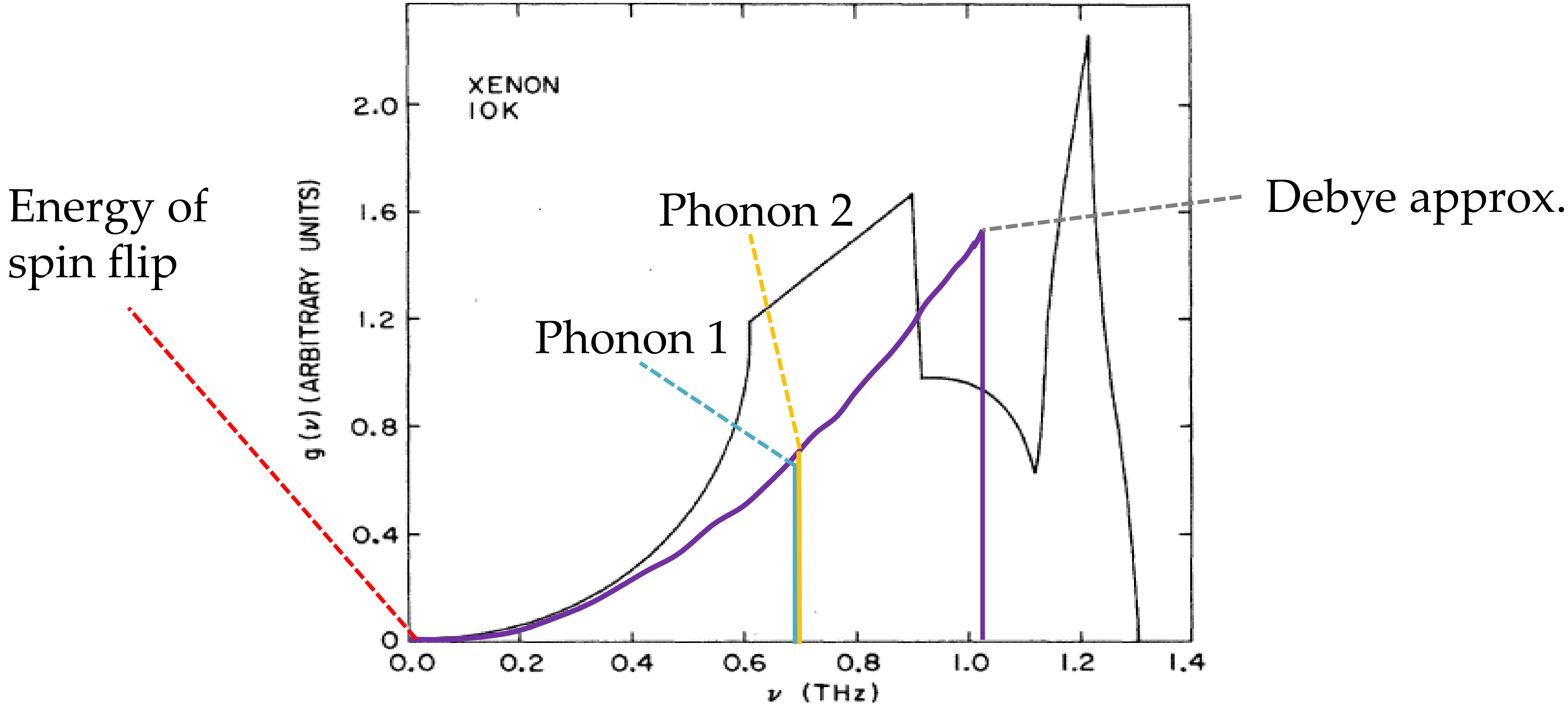

FIG. 2. Density-of-states function for xenon at 10 K, normalized to unit area.

–Lurie, et al., PRB (1974)

Theory: Solid ^{129}Xe Relaxation

– 1R, Fitzgerarld, et al., PRB (1999)

$$\frac{c_{K0}}{h} = \left(\frac{\mu_K}{K\mu_B}\right)\left(\frac{\hbar}{8\pi M R_0^2}\right)(\sigma_g - \sigma_c)$$

$$\frac{c_{K0}}{h} = -27 \text{ Hz}$$

$$\nu = \frac{c_K}{\hbar}\mathbf{K}\cdot\mathsf{I}\cdot\boldsymbol{\omega} = c_K \mathbf{K}\cdot\mathbf{N}$$

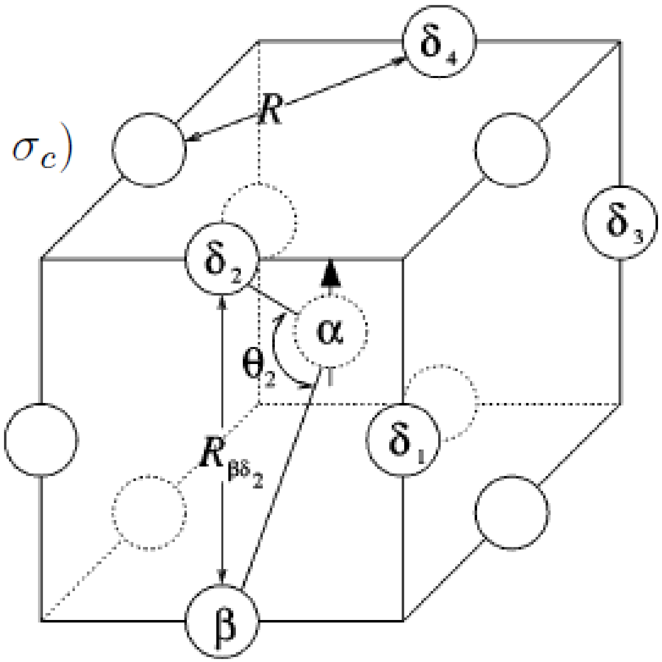

Theory: Solid ^{129}Xe Relaxation

– 1R, Fitzgerarld, et al., PRB (1999)

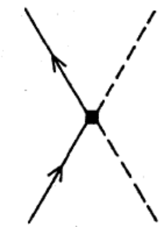

$$\frac{1}{T_1^S} = \frac{9\hbar^2\mu_K^2(\sigma_g-\sigma_c)^2}{256\pi K^2\mu_B^2 M^2 R_0^2 T_D^2}\sum_m g_m\left(4+\frac{8}{3}\epsilon_0+\frac{1}{3}\epsilon_0^2(2\cos^2\theta_m+1)\right)$$

$$\times\int_0^1 du\, u^4\frac{e^{\frac{uT_D}{T}}}{\left(e^{\frac{uT_D}{T}}-1\right)^2}\left[1+\mathrm{sinc}\left(u\sigma_m(6\pi^2\sqrt{2})^{\frac{1}{3}}\right)+\mathrm{sinc}\left(u(6\pi^2\sqrt{2})^{\frac{1}{3}}\right)\right]^2$$

$$\frac{c_{K0}}{h}=\left(\frac{\mu_K}{K\mu_B}\right)\left(\frac{\hbar}{8\pi M R_0^2}\right)(\sigma_g-\sigma_c)$$

$$\frac{c_{K0}}{h}=-27\text{ Hz}$$

$$\nu=\frac{c_K}{\hbar}\mathbf{K}\cdot\mathsf{I}\cdot\boldsymbol{\omega}=c_K\mathbf{K}\cdot\mathbf{N}$$

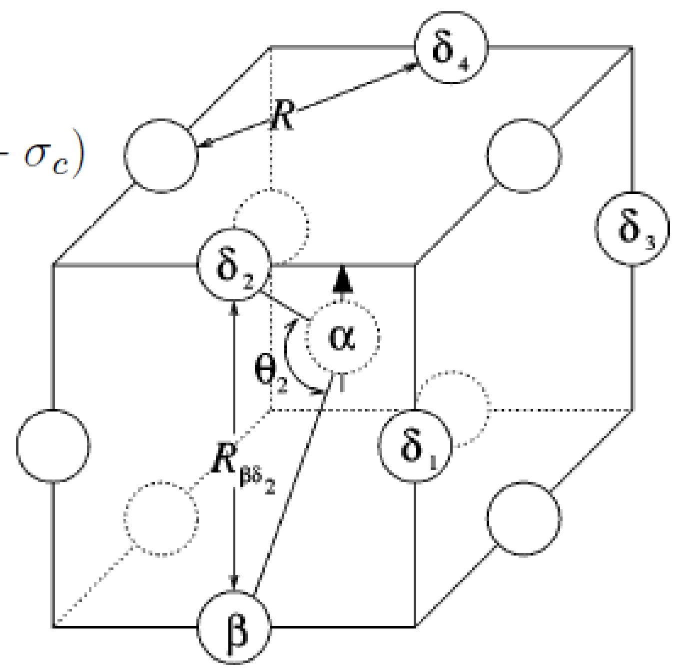

$$\epsilon = R\frac{d}{dR}\ln c_K$$

m	g_m	σ_m	$\cos(\theta_m)$
0	12	$\sqrt{0}$	1
1	48	$\sqrt{1}$	1/2
2	24	$\sqrt{2}$	0
3	48	$\sqrt{3}$	-1/2
4	12	$\sqrt{4}$	-1

Theory: Solid ^{129}Xe Relaxation

– 1R, Fitzgerarld, et al., PRB (1999)

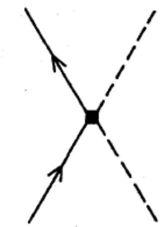

$$\frac{1}{T_1^S} = \boxed{\frac{9\hbar^2\mu_K^2(\sigma_g-\sigma_c)^2}{256\pi K^2\mu_B^2 M^2 R_0^2 T_D^2}} \sum_m g_m \left(4+\frac{8}{3}\epsilon_0+\frac{1}{3}\epsilon_0^2(2\cos^2\theta_m+1)\right)$$

$$\times \int_0^1 du\; u^4 \boxed{\frac{e^{\frac{uT_D}{T}}}{\left(e^{\frac{uT_D}{T}}-1\right)^2}} \boxed{\left[1+\mathrm{sinc}\left(u\sigma_m(6\pi^2\sqrt{2})^{\frac{1}{3}}\right)+\mathrm{sinc}\left(u(6\pi^2\sqrt{2})^{\frac{1}{3}}\right)\right]^2}$$

Temperature dependence

Conservation of momentum

$$\boxed{\frac{c_{K0}}{h} = -27\text{ Hz}}$$

Spin-rotation coupling strength

Hanni, c_{K0}/h = -16 Hz

Theory: Solid ^{129}Xe Relaxation

– Fermi's golden rule

$$dW_{fi} = \frac{2\pi}{\hbar}|\nu_{fi}|^2 \rho(E_e) d\Omega_e$$

$$\nu = \sum_\beta c_K(R_{\beta\alpha}) \mathbf{N}_{\beta\alpha} \cdot \mathbf{K}$$
$$= \frac{1}{2\hbar} \sum_\beta c_K(R_{\beta\alpha}) \mathbf{R}_{\beta\alpha} \times \mathbf{P}_{\beta\alpha} \cdot \mathbf{K}$$

Theory: Solid ^{129}Xe Relaxation

– Fermi's golden rule

$$dW_{fi} = \frac{2\pi}{\hbar}|\nu_{fi}|^2\rho(E_e)d\Omega_e$$

$$\nu = \sum_\beta c_K(R_{\beta\alpha})\mathbf{N}_{\beta\alpha}\cdot\mathbf{K}$$
$$= \frac{1}{2\hbar}\sum_\beta c_K(R_{\beta\alpha})\mathbf{R}_{\beta\alpha}\times\mathbf{P}_{\beta\alpha}\cdot\mathbf{K}$$

– Initial and final states

$$|i\rangle = |m_K = 1/2; \ldots, n_{\mathbf{k}_a j_a}, n_{\mathbf{k}_e j_e}, \ldots\rangle\,,$$

$$|f\rangle = |m_K = -1/2; \ldots, n_{\mathbf{k}_a j_a} - 1, n_{\mathbf{k}_e j_e} + 1, \ldots\rangle$$

Theory: Solid ^{129}Xe Relaxation

– Fermi's golden rule

$$dW_{fi} = \frac{2\pi}{\hbar}|\nu_{fi}|^2\rho(E_e)d\Omega_e$$

$$\nu = \sum_\beta c_K(R_{\beta\alpha})\mathbf{N}_{\beta\alpha}\cdot\mathbf{K}$$
$$= \frac{1}{2\hbar}\sum_\beta c_K(R_{\beta\alpha})\mathbf{R}_{\beta\alpha}\times\mathbf{P}_{\beta\alpha}\cdot\mathbf{K}$$

– Initial and final states

$$|i\rangle = |m_K = 1/2; \ldots, n_{\mathbf{k}_a j_a}, n_{\mathbf{k}_e j_e}, \ldots\rangle\,,$$

$$|f\rangle = |m_K = -1/2; \ldots, n_{\mathbf{k}_a j_a} - 1, n_{\mathbf{k}_e j_e} + 1, \ldots\rangle$$

– Canonical quantization $\mathbf{R}_\nu = \mathbf{R}_\nu^{(0)} + \mathbf{S}_\nu$

$$\mathbf{S}_\nu = \sqrt{\frac{\hbar}{2NMc_s}}\sum_{\mathbf{k}j}\frac{\mathbf{x}_j}{\sqrt{k}}\left[a_{\mathbf{k}j}e^{i\mathbf{k}\cdot\mathbf{R}_\nu^{(0)}} + a_{\mathbf{k}j}^\dagger e^{-i\mathbf{k}\cdot\mathbf{R}_\nu^{(0)}}\right]$$

$$\mathbf{P}_\nu = \sqrt{\frac{\hbar Mc_s}{2N}}\sum_{\mathbf{k}j}\sqrt{k}\mathbf{x}_j\left[ia_{\mathbf{k}j}^\dagger e^{-i\mathbf{k}\cdot\mathbf{R}_\nu^{(0)}} - ia_{\mathbf{k}j}e^{i\mathbf{k}\cdot\mathbf{R}_\nu^{(0)}}\right]$$

Theory: Solid ^{129}Xe Relaxation

- At high temp., temp. dependence comes from only phonon occupation numbers, *n*

$$|\langle n_i - 1, n_j + 1|\, a_i a_j^\dagger \,|n_i, n_j\rangle|^2 = n_i(n_j + 1)$$

Fermi's golden rule

- These occupation numbers are averaged over using a Bose-Einstein distribution

$$< n_i >< n_j + 1 >= \frac{1}{e^{x/T} - 1} \frac{e^{x/T}}{e^{x/T} - 1}$$

Theory: Solid ^{129}Xe Relaxation

– Which appears exactly in T_1 formula

$$\frac{1}{T_1^S} = \frac{9\hbar^2\mu_K^2(\sigma_g-\sigma_c)^2}{256\pi K^2\mu_B^2 M^2 R_0^2 T_D^2}\sum_m g_m\left(4+\frac{8}{3}\epsilon_0+\frac{1}{3}\epsilon_0^2(2\cos^2\theta_m+1)\right)$$
$$\times\int_0^1 du\ u^4\boxed{\frac{e^{\frac{uT_D}{T}}}{\left(e^{\frac{uT_D}{T}}-1\right)^2}}\left[1+\mathrm{sinc}\left(u\sigma_m(6\pi^2\sqrt{2})^{\frac{1}{3}}\right)+\mathrm{sinc}\left(u(6\pi^2\sqrt{2})^{\frac{1}{3}}\right)\right]^2$$

$$\boxed{< n_i >< n_j + 1 >= \frac{1}{e^{x/T}-1}\frac{e^{x/T}}{e^{x/T}-1}}$$

Theory: Solid ^{129}Xe Relaxation

– At high temp. (higher than Debye temp., 55 K), each unique *n* contributes *T*

$$< n_i >< n_j + 1 >= \frac{1}{e^{x/T}-1}\frac{e^{x/T}}{e^{x/T}-1}$$
$$\rightarrow \frac{1}{1+x/T-1}\frac{1}{1+x/T-1} \propto T * T$$

Theory: Solid ^{129}Xe Relaxation

– The third phonon's occupation number in the aR process drops out, T^2 remains

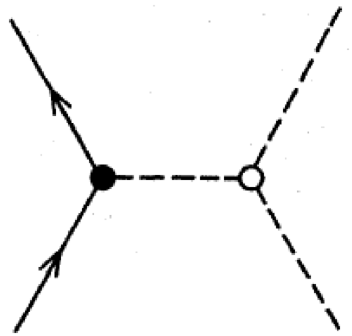

$$< n_i >< n_j + 1 >= \frac{1}{e^{x/T}-1}\frac{e^{x/T}}{e^{x/T}-1}$$

$$\to \frac{1}{1+x/T-1}\frac{1}{1+x/T-1} \propto T * T$$

Theory: Solid ^{129}Xe Relaxation

– Irrespective of mechanism, any *generic* process has a temp. dependence defined by the number of unique external phonons

$$\langle n_1 \rangle \cdots \langle n_i \rangle \propto T^i \quad \text{(High-temp.)}$$

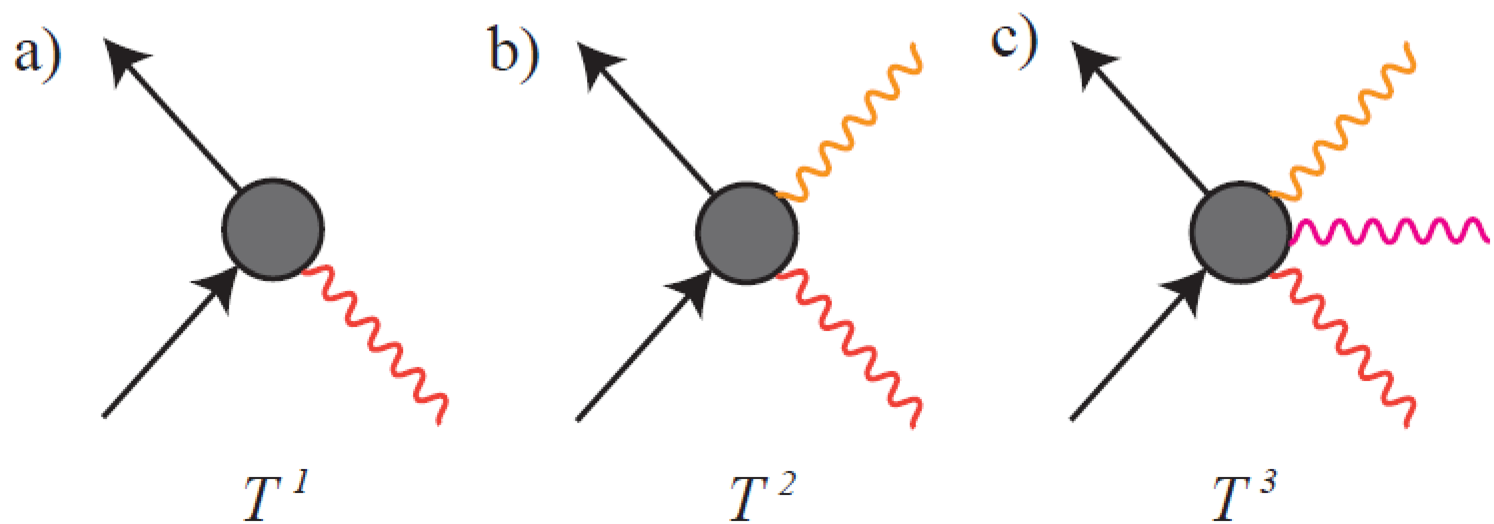

Theory: Solid ^{129}Xe Relaxation

- Though energy conservation is violated, consider non-unique phonon case

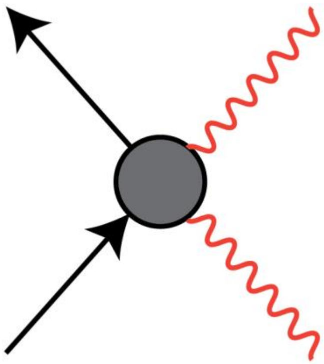

$$|\langle n|\, a^\dagger a\, |n\rangle|^2 = n^2$$

Fermi's golden rule

$$\langle n^2 \rangle = \langle n \rangle + 2\langle n \rangle^2 \propto T + 2T^2$$

(High-temp.)

Theory: Solid ^{129}Xe Relaxation

– In scattering problems, conservation of momentum is more strict than energy

$$W_{fi} = \frac{2\pi}{\hbar} \sum_{j_e j_a} \int_0^{E_D} dE_a \boxed{d\Omega_a d\Omega_e} |v_{fi}|^2 \rho^2(E_a)$$

– Typically in phonon scattering, a sum over entire lattice generates a delta function

$$\frac{1}{N} \sum_l e^{i\mathbf{r}^l \cdot (\mathbf{k_1} - \mathbf{k_2})} = \Delta(\mathbf{k_1} - \mathbf{k_2})$$

$$\Delta(\mathbf{k}) = \begin{cases} 1 & \text{if } \mathbf{k} = \mathbf{G}, \\ 0 & \text{otherwise.} \end{cases}$$

Theory: Solid ^{129}Xe Relaxation

– Momentum conservation leads to a sizable difference

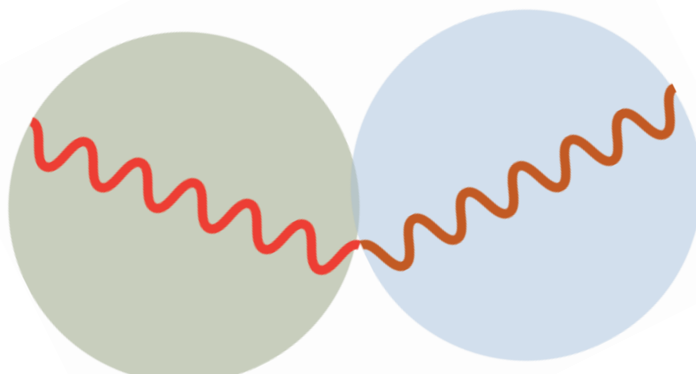

$$T_1 = 300 \text{ min.}$$

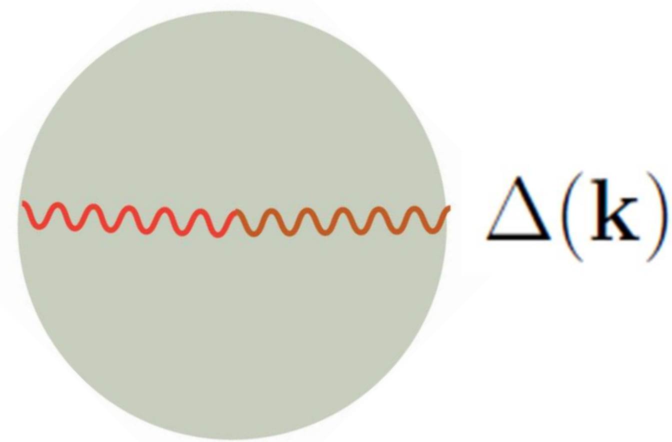

$$T_1 = 1500 \text{ min.}$$

(Using Hanni/h, c_{K0} = -16 Hz)

Open: Solid ^{129}Xe Relaxation

– Much future work, reopens field

– Create a structure-dependent theory

– Determine conservation of momentum

– Get lower temp. ice data, single crystal(?)

– Snow, experiments and theory

Finished: Solid ^{129}Xe Relaxation

- Developed ice method that allows for unprecedented, robust T_1 data
- Discovered intrinsic difference between bulk snow and ice
- Found generic high-temp. T_1 behavior
- Found structural dependence in dilute T_2

Unconventional MR

Semiconductor ODMR/EDMR

- Optically Detected MR, Electrically Detected MR; dipolar and exchange

- Permutation symmetry of paramagnetic pairs determines signal, not polarization

$$|\uparrow\uparrow\rangle$$
$$\cos(\phi)\,|\uparrow\downarrow\rangle - \sin(\phi)\,|\downarrow\uparrow\rangle$$
$$\cos(\phi)\,|\uparrow\downarrow\rangle + \sin(\phi)\,|\downarrow\uparrow\rangle$$
$$|\downarrow\downarrow\rangle$$

Semiconductor ODMR/EDMR

– Resonate spin-1/2 pair, detect the optical or electrical deviation from steady state

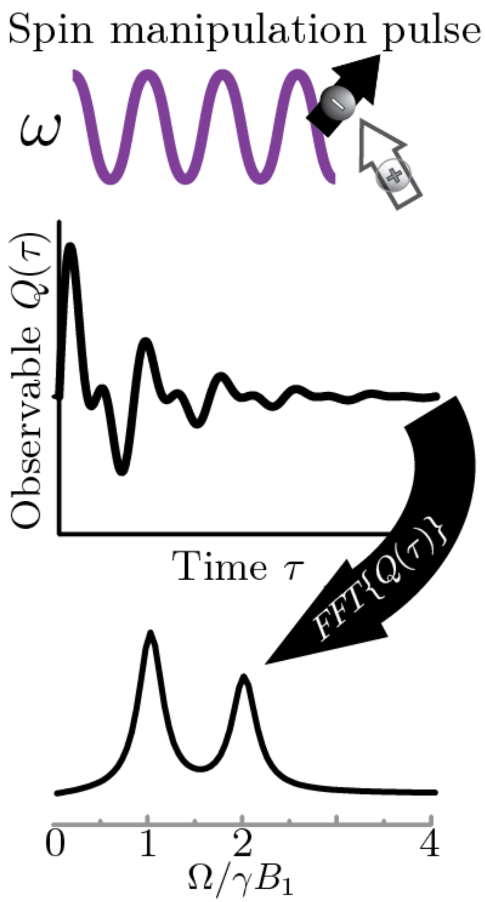

Semiconductor ODMR/EDMR

– Repeat for detuned pulses

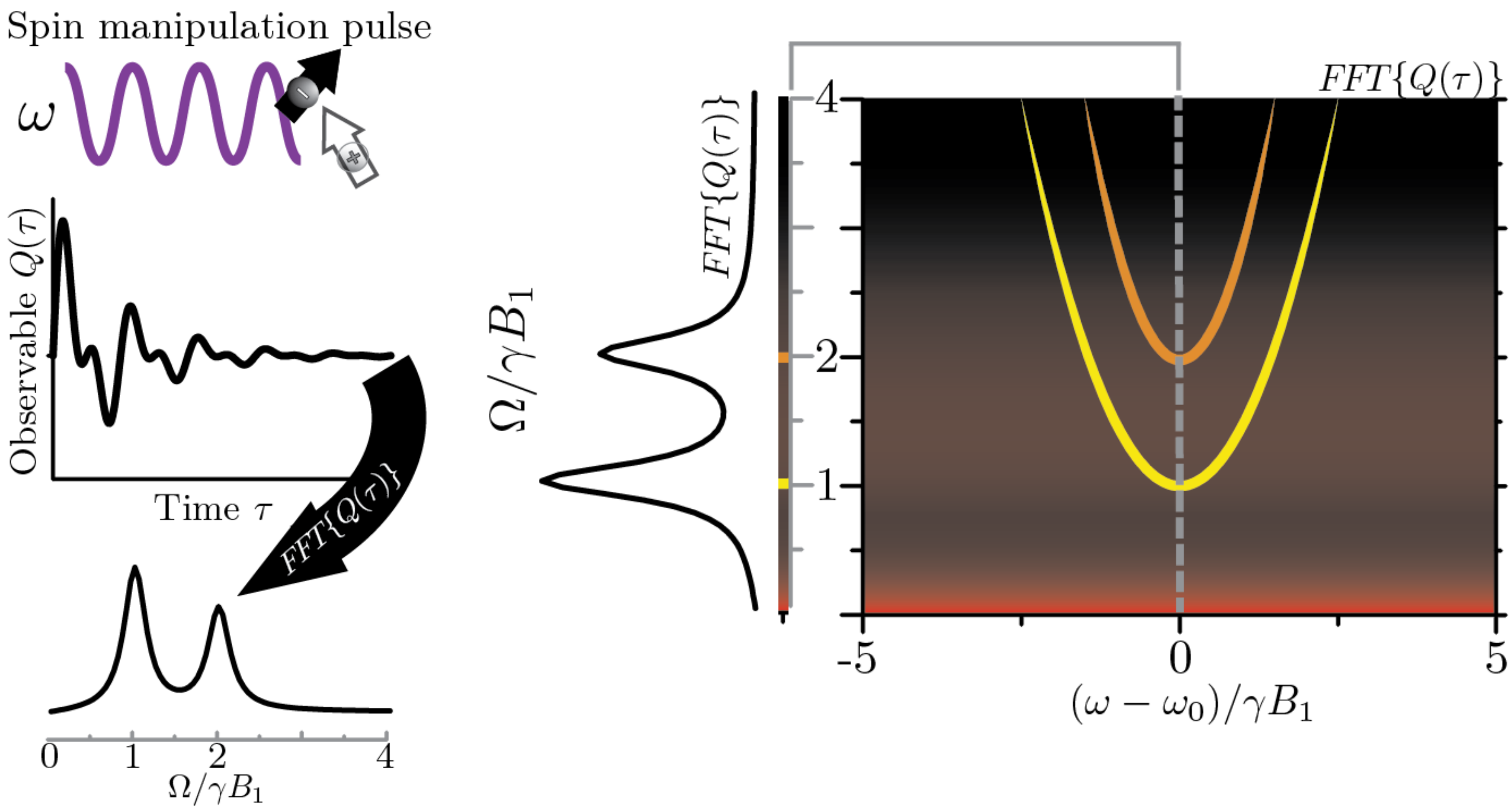

Semiconductor ODMR/EDMR

– Implemented Liouville-space formalism, allowing for quick computation of inhomogeneous, stochastic Liouville equation, for dipolar and exchange coupled pairs

$$\rho = \begin{array}{c c} & \begin{array}{cc} \langle\uparrow| & \langle\downarrow| \end{array} \\ \begin{array}{c} |\uparrow\rangle \\ |\downarrow\rangle \end{array} & \begin{pmatrix} \rho_{11} & \rho_{12} \\ \rho_{21} & \rho_{22} \end{pmatrix} \end{array} \qquad \rho = \begin{pmatrix} \rho_{11} \\ \rho_{12} \\ \rho_{21} \\ \rho_{22} \end{pmatrix}$$

Generation takes 10 min. instead of 7 days.

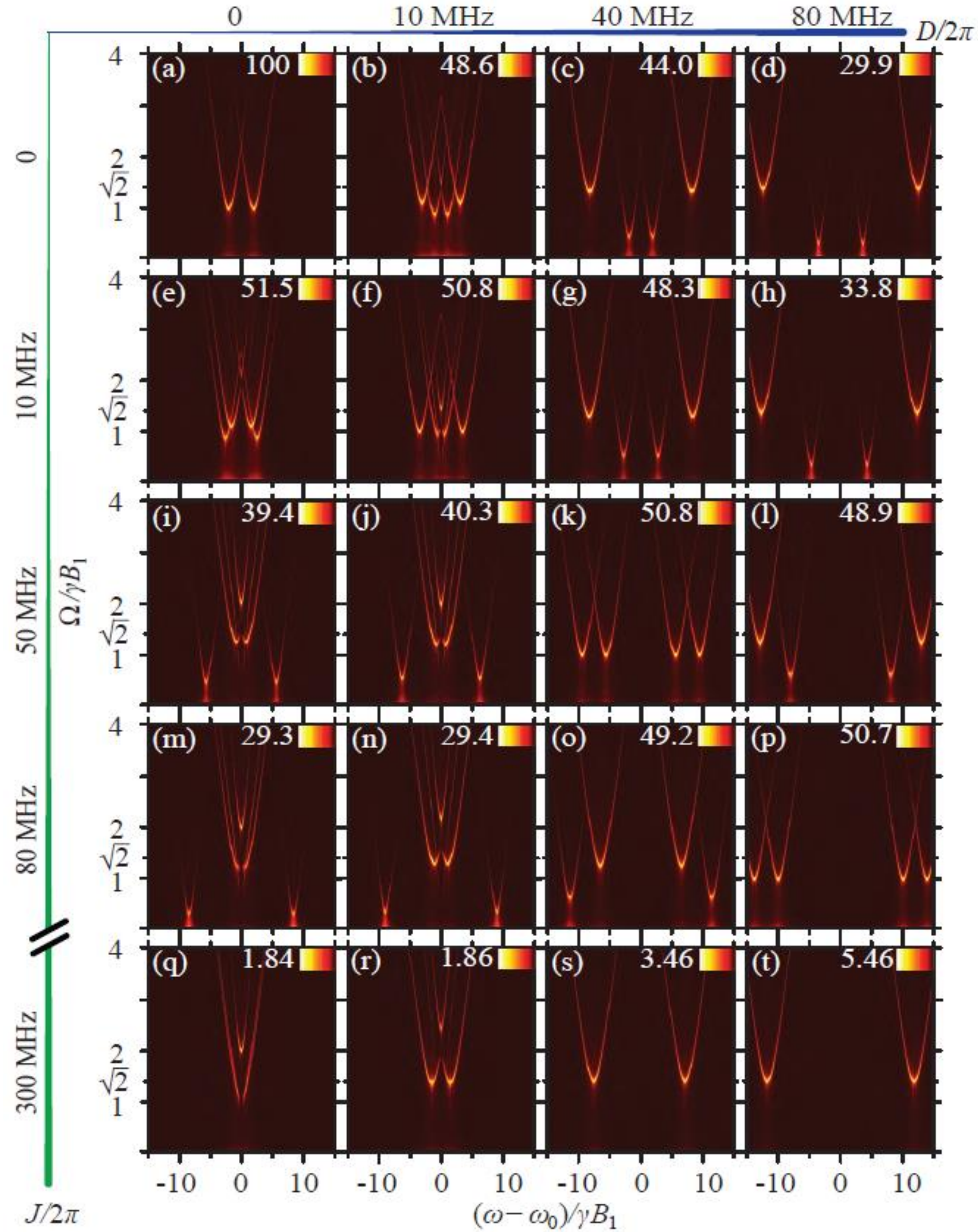

Limes, et al., PRB (2013)

Semiconductor ODMR/EDMR

– Showed that single-transition Rabi frequencies are given by

$$\Omega_{ij} = \sqrt{(1 \mp \sin 2\phi)\,(\gamma B_1)^2 + (\omega - \omega_{ij})^2}$$

and with sufficient dipolar coupling,

$$\sin 2\phi \rightarrow -1$$

leading to an on-resonant Rabi frequency

$$\sqrt{2}\gamma B_1$$

Mixed MR

B_0 modulation

– Apply a B_0 modulation field, $B_2{}'$

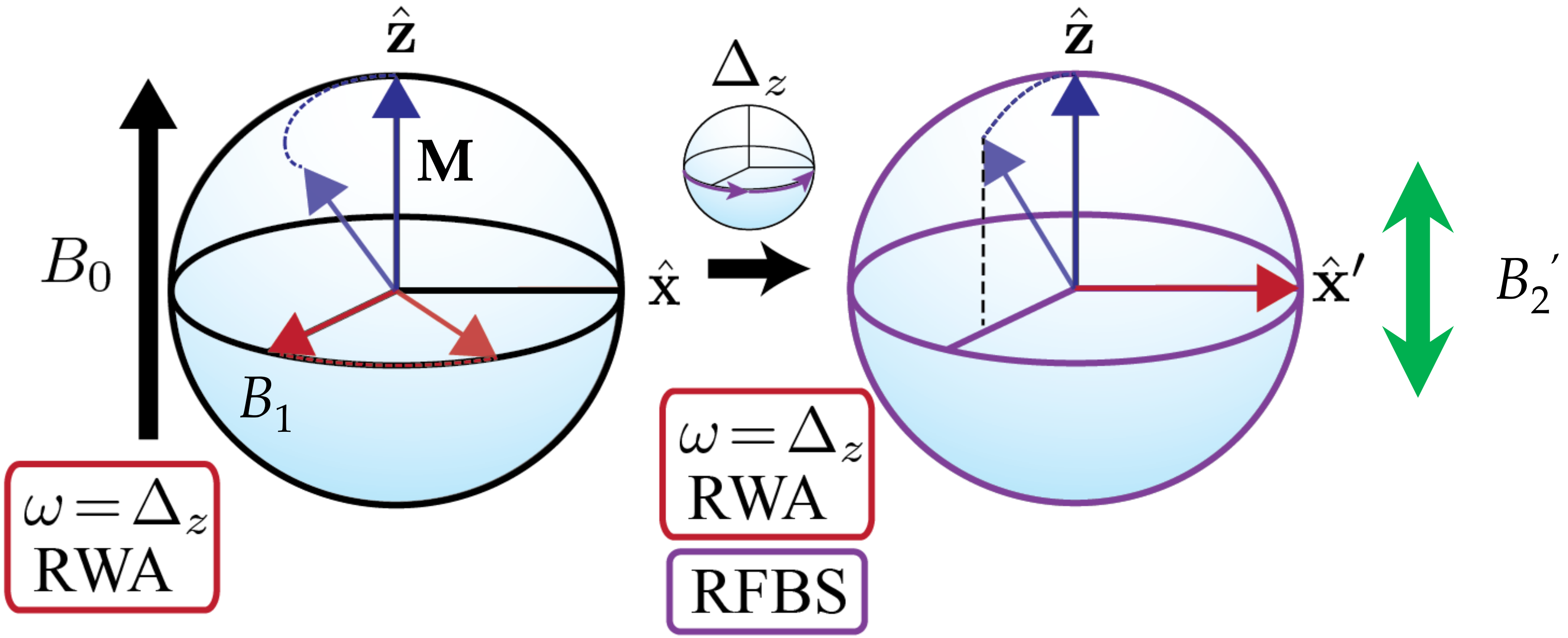

B_0 modulation

– Readjust for comfort, quantization x′-axis

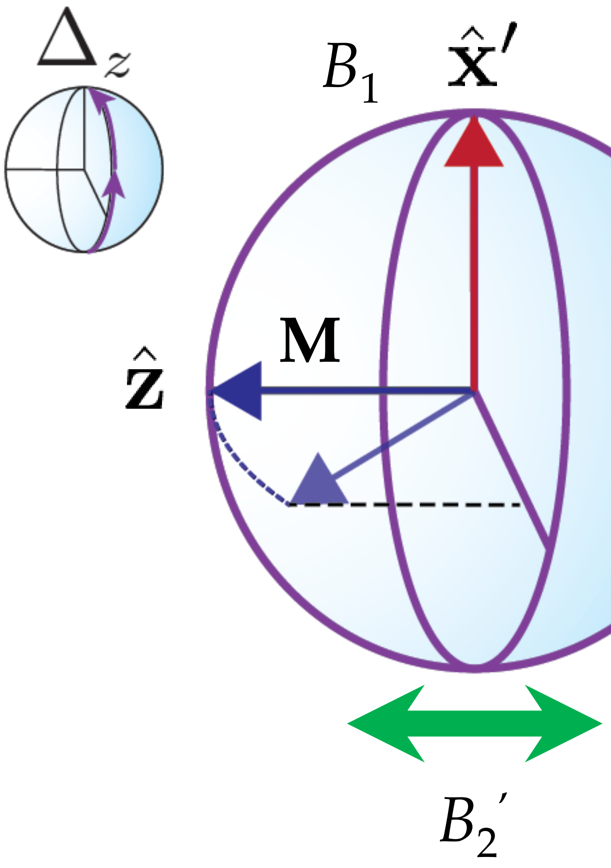

B_0 modulation

– Access unconventional regimes, $B_2 >> B_1$

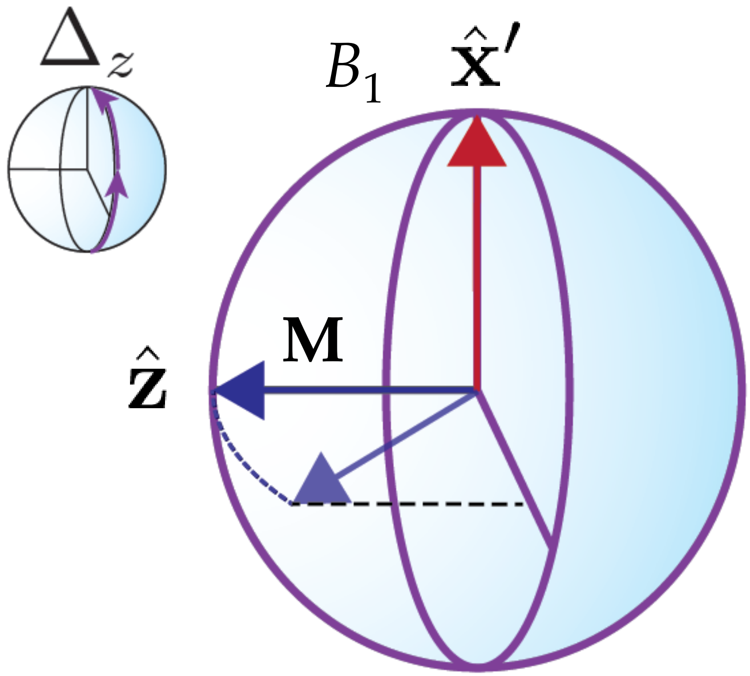

Relatively high polarization

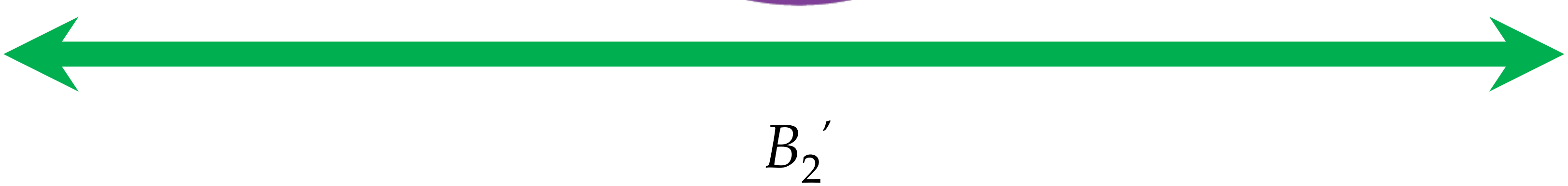

B_0 modulation

– Determine Rabi envelope dynamics $B_1 \gg B_2$

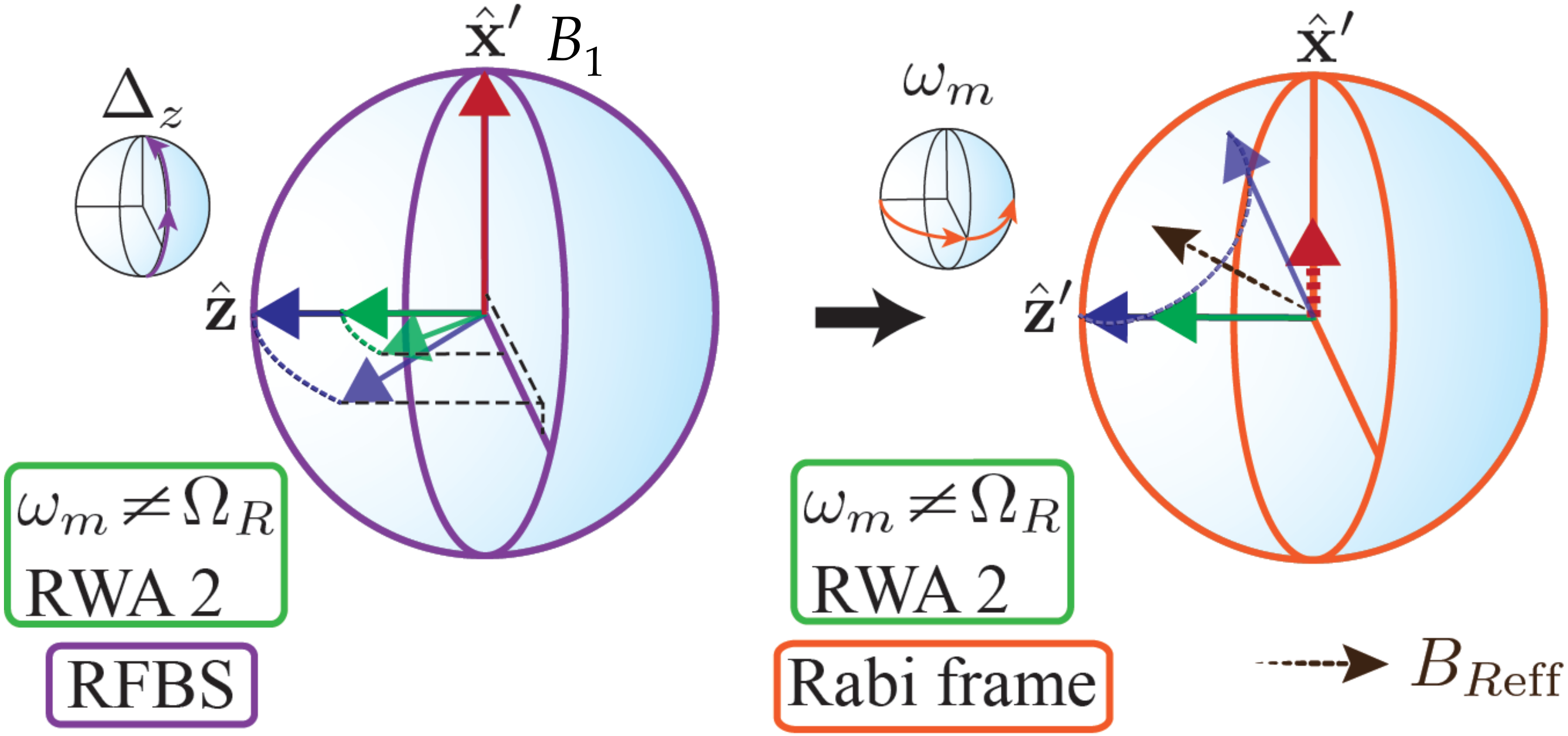

B_0 modulation

– Regime: weak-resonant modulation

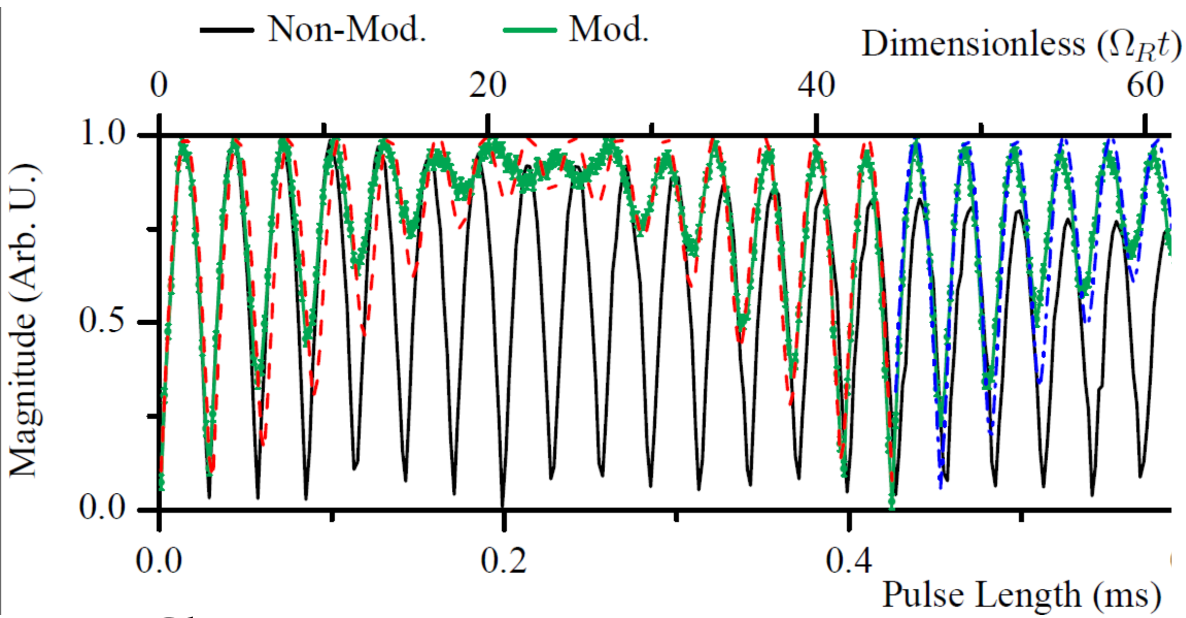

Glenn, Limes,
et al., PRB (2013)

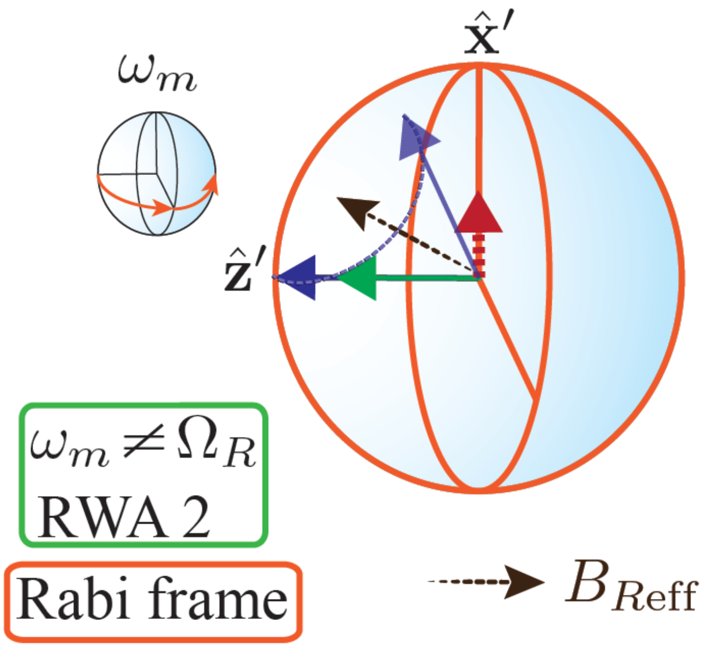

Overview

- Magnetic Resonance
  - Conventional (NMR)
    - Solid ^{129}Xe Relaxation
  - Unconventional (ODMR/EDMR)
    - Dipolar Coupling $\Omega_R = \sqrt{2}\Omega$
  - Mixed (B_0 modulation)
    - Three regimes Rabi frame

THE UNIVERSITY OF UTAH

Acknowledgements/Work

Back Row: Zayd Ma, Haleigh Emerson, Elliot Nielson, Eddie Thenell
Front Row: David Ailion, Brian Saam, Gernot Laicher, Mark Limes, Hans Malissa
Not pictured: Kyle Jeong, Tom Paskvan











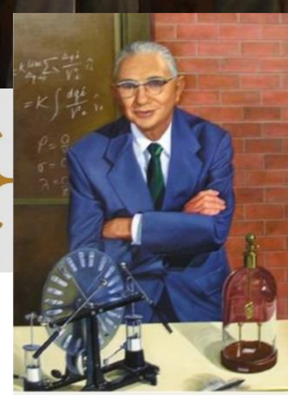

J. Irvin Swigart

NATIONAL SCIENCE FOUNDATION MRSEC MATERIALS RESEARCH SCIENCE & ENGINEERING CENTERS

Acknowledgements/Home



Acknowledgements/Heidi

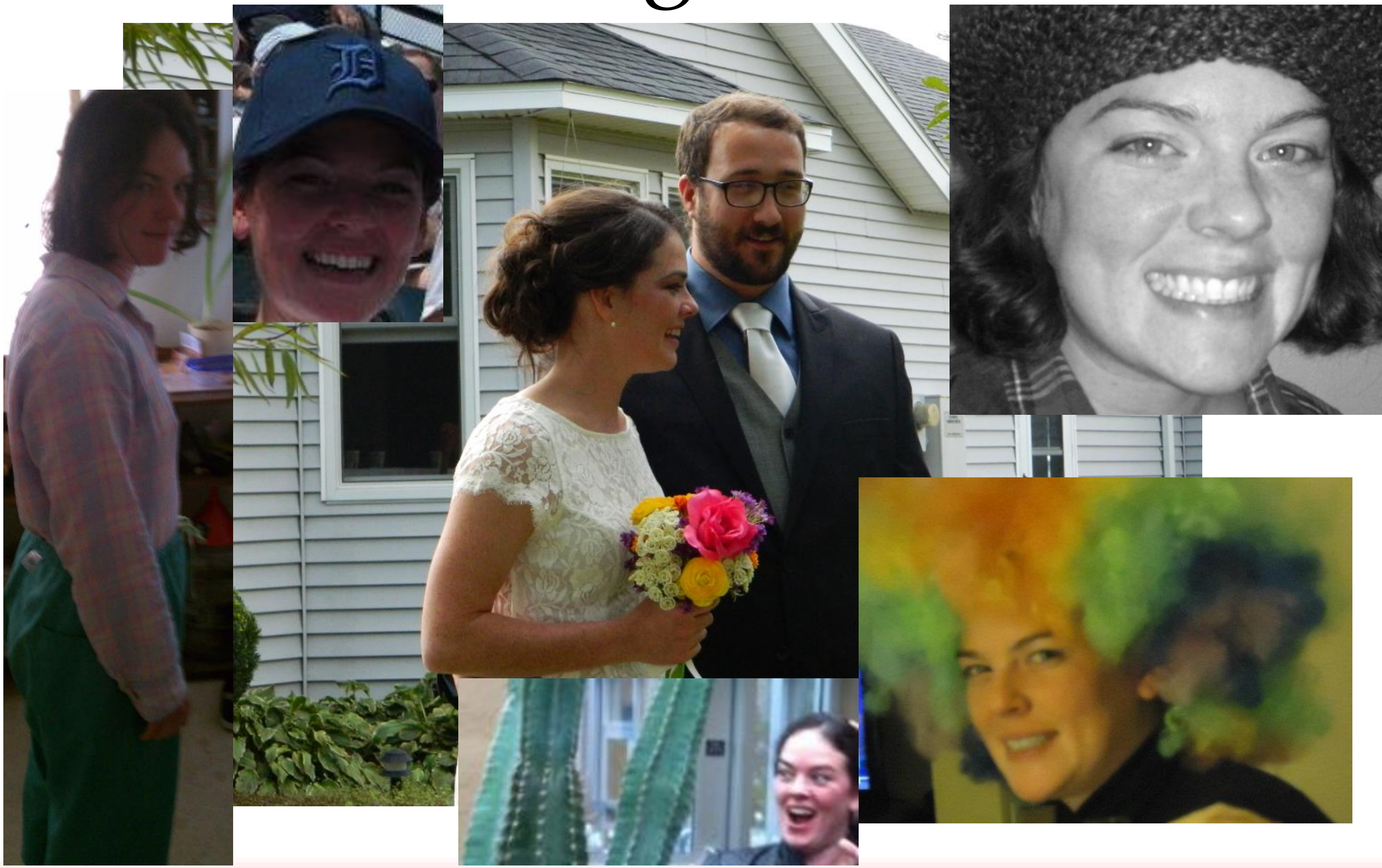


UTAH

fin